年性の場合には寝具やカーペット，エアコンなどのダニ，ハウスダスト対策が必要となる．

III. アトピー性角結膜炎と春季カタル

1. 概念と原因

分類の項で述べたように，アトピー性皮膚炎に合併したアレルギー性結膜炎は増殖性変化を伴うことが多いし，春季カタルの約半数はアトピー性皮膚炎を合併している．このため，ここでは両者を一括して述べる．

アトピー性皮膚炎で，顔面に皮膚症状の強い例では多かれ少なかれアレルギー性結膜炎を合併していることが多い．眼瞼皮膚にはアトピー性乾燥肌，色素沈着が見られ，高率に眼瞼炎を合併する．重症例では眼瞼皮膚の硬化が強くなり，睫毛乱生や閉瞼不全を伴うようになる(図3)．アトピー性皮膚炎のアレルゲンとしてはダニとハウスダストが圧倒的に多いことが知られている．

2. 症状と所見

[小児の特性]
- アトピー性皮膚炎重症例ではアレルギー性結膜炎を高率に合併する
- 角膜障害を伴う重症例は学童期の小児に多い

アトピー性皮膚炎では，眼症状のない患児の場合でも，診察してみると上眼瞼結膜に乳頭増殖が見られることが多い(図4)．乳頭の直径が1 mm以上の場合を巨大乳頭と呼び，増殖性変化があると判定される．分類上はここがアトピー性角結膜炎と春季カタルの境界ということになる．

アトピー性角結膜炎や春季カタルは慢性のアレルギー性疾患であり，好酸球が主体をなすI型アレルギー遅発相が関与するところがアレルギー性結膜炎との大きな違いである．好酸球から放出されるmajor basic proteinなどの組織障害性蛋白が角膜や結膜を障害する．これによって点状表層角膜症や落屑様角膜上皮障害，シールド潰瘍が出現するほか，結膜障害の異常修復であるリモデリングにより巨大乳頭，石垣状の乳頭増殖が形成される(図5)．また，結膜の増殖性変化のもう一つの形である輪部結膜の腫脹や堤防状隆起が生じることもあり(図6)，前者を眼瞼型，後者を眼球型

図3 アトピー性皮膚炎
眼瞼皮膚の硬化が強く，閉瞼不全を伴っている．

図4 アトピー性角結膜炎
原則的に結膜の増殖性変化を伴わないが，上眼瞼結膜に乳頭増殖が見られることもある．

図5 春季カタル
石垣状の乳頭増殖．充血が強く，乳頭の谷間に粘性の眼脂が見られるのは活動性が高いことを示す．

(輪部型)の春季カタルと呼ぶ.

春季カタルで見られる角膜合併症の重症型がシールド潰瘍である(図7). シールド潰瘍は角膜中央部から上方にみられる円形または楕円形の浅い潰瘍で, 潰瘍底が白色に混濁しているのが特徴である. 潰瘍底にムチンや変性上皮, カルシウム塩などが蓄積すると角膜プラークとなる.

3. 治療

[プライマリケアでの治療指針の立て方]
- ベースとしての抗アレルギー薬の点眼は必須
- 病勢の強い時期にはステロイド剤の点眼を積極的に用いる
- 病勢が落ち着いてきたらシクロスポリンにスイッチしていく
- シールド潰瘍を伴う重症例は可能なら専門医に紹介する

アトピー性角結膜炎で, 自覚症状や炎症所見が強くない例ではアレルギー性結膜炎の治療に準じて良い. I型アレルギー遅発相が関与するといっても, 肥満細胞が主役であるI型アレルギー即時相が根底にあるので, 病勢全体のコントロールのために抗アレルギー薬の点眼は必要である.

角膜上皮障害を伴う例, 特にシールド潰瘍を伴うような重症例では, ステロイド薬の点眼が必要であり, 場合によってはトリアムシノロンの瞼板下注射を行う. 免疫抑制薬であるシクロスポリンの点眼薬も有用であるが, 即効性に乏しいので, まずステロイド薬で病勢を抑えて, うまくシクロスポリンの点眼にスイッチしていくのがコツであろうと思われる. 角膜プラークが見られる場合には, 薬物療法では治癒しにくいので, メスなどで外科的に除去する必要がある. 筆者自身は, 病勢が落ち着いてプラークが固い感じになってから, 鑷子でつまんで鈍的に除去することを好んでいる.

春季カタルの病勢の強さは, 瞼結膜の乳頭の充血の強さと乳頭間の眼脂をみるとわかりやすい.

図6 春季カタル
輪部結膜の腫脹, 堤防状隆起があり, 眼球型である.

図7 シールド潰瘍
円形または楕円形の浅い潰瘍で, 潰瘍底が白色に混濁している.

病勢が落ち着いていると乳頭も徐々に縮小していくが, これにはかなりの時間を要する. どうしても炎症がコントロールできない場合には, ステロイド薬の内服を短期間行うか, 結膜乳頭の外科的切除や冷凍凝固を行うとよい.

[文献]
1) 熊谷直樹：アレルギー性結膜炎患者の疫学. 日本の眼科 69：905-909, 1998
2) 日本眼科アレルギー研究会：アレルギー性結膜疾患診療ガイドライン. 日眼会誌 110：99-140, 2006
3) 稲田紀子：アレルギー疾患. 眼科 47：1588-1595, 2005

JOURNAL OF BACTERIOLOGY, Aug. 2007, p. 5749–5761 Vol. 189, No. 15
0021-9193/07/$08.00+0 doi:10.1128/JB.00194-07

Molecular Characterization of Membrane-Associated Soluble Serine Palmitoyltransferases from *Sphingobacterium multivorum* and *Bdellovibrio stolpii*[▽]

Hiroko Ikushiro,[1]* Mohammad Mainul Islam,[1]† Hiromasa Tojo,[2] and Hideyuki Hayashi[1]*

Department of Biochemistry, Osaka Medical College, Takatsuki, Osaka 569-8686, Japan,[1] and Department of Biochemistry and Molecular Biology, Osaka University, Graduate School of Medicine, 2-2 Yamadaoka, Suita, Osaka 565-0871, Japan[2]

Received 5 February 2007/Accepted 10 May 2007

Serine palmitoyltransferase (SPT) is a key enzyme in sphingolipid biosynthesis and catalyzes the decarboxylative condensation of L-serine and palmitoyl coenzyme A (CoA) to form 3-ketodihydrosphingosine (KDS). Eukaryotic SPTs comprise tightly membrane-associated heterodimers belonging to the pyridoxal 5′-phosphate (PLP)-dependent α-oxamine synthase family. *Sphingomonas paucimobilis*, a sphingolipid-containing bacterium, contains an abundant water-soluble homodimeric SPT of the same family (H. Ikushiro et al., J. Biol. Chem. 276:18249–18256, 2001). This enzyme is suitable for the detailed mechanistic studies of SPT, although single crystals appropriate for high-resolution crystallography have not yet been obtained. We have now isolated three novel SPT genes from *Sphingobacterium multivorum*, *Sphingobacterium spiritivorum*, and *Bdellovibrio stolpii*, respectively. Each gene product exhibits an ~30% sequence identity to both eukaryotic subunits, and the putative catalytic amino acid residues are conserved. All bacterial SPTs were successfully overproduced in *Escherichia coli* and purified as water-soluble active homodimers. The spectroscopic properties of the purified SPTs are characteristic of PLP-dependent enzymes. The KDS formation by the bacterial SPTs was confirmed by high-performance liquid chromatography/mass spectrometry. The *Sphingobacterium* SPTs obeyed normal steady-state ordered Bi-Bi kinetics, while the *Bdellovibrio* SPT underwent a remarkable substrate inhibition at palmitoyl CoA concentrations higher than 100 μM, as does the eukaryotic enzyme. Immunoelectron microscopy showed that unlike the cytosolic *Sphingomonas* SPT, *S. multivorum* and *Bdellovibrio* SPTs were bound to the inner membrane of cells as peripheral membrane proteins, indicating that these enzymes can be a prokaryotic model mimicking the membrane-associated eukaryotic SPT.

Sphingolipids are ubiquitous membrane components of the eukaryotic plasma membrane (32) and are known to be essential lipidic signaling molecules required for various cellular events, such as proliferation, differentiation, and apoptosis (22, 38, 54). In addition, sphingolipids together with cholesterol are the major components of the membrane microdomains called "lipid rafts," which serve as platforms for signal transduction or the transport of various bioactive molecules via membrane trafficking (14, 25, 52).

Serine palmitoyltransferase (SPT) (EC 2.3.1.50) catalyzes the pyridoxal 5′-phosphate (PLP)-dependent condensation reaction of L-serine with palmitoyl coenzyme A (CoA) to generate 3-ketodihydrosphingosine (KDS). This reaction is the first committed step in the de novo biosynthetic pathway of all sphingolipids, producing long-chain bases (LCBs), the backbone structure of sphingolipids. SPT is thought to be the key enzyme regulating the cellular sphingolipid content (21). Eukaryotic SPTs are enriched in the endoplasmic reticulum, with their catalytic sites facing the cytosol (36), and function as heterodimers comprising two tightly membrane-bound subunits, called LCB1 and LCB2, which share a sequence similarity (~25% identity) (10, 19, 20, 41, 42, 64). Recently a new subunit protein of the human SPT, SPTLC3, was found (24). Due to the high sequence similarity (68% identity) between SPTLC2 (LCB2 subunit of human SPT) and SPTLC3, SPTLC3 is thought to form a dimer with SPTLC1. LCB2 (SPTLC2) and SPTLC3 are the putative catalytic subunits carrying a lysine residue that forms the Schiff base with PLP. In contrast, LCB1 does not have such a motif (10, 19) and does not seem to function as the catalytic center. Nevertheless, LCB1 is regarded to be essential for the catalytic action of SPT (20), and mutations in the LCB1 gene are known to cause human hereditary sensory neuropathy type I (HSN1) (6, 11, 61). The roles of SPT activity in the pathogenesis of HSN1, however, are elusive at present (7, 17, 40). Elucidation of the structure-activity relationship of SPT is essential for understanding the role of the rate-limiting enzyme, SPT, in regulating the cellular sphingolipid homeostasis and for clarifying the underlying causes of HSNI. There is, however, little structural and mechanistic information on the mammalian SPT currently available, because the instability and the hydrophobic nature of each subunit have hindered the successful purification of recombinant SPT for crystallization and structural analysis (26).

Previously we found and isolated a water-soluble homodimeric SPT from *Sphingomonas paucimobilis* EY2395[T] (27). The *Sphingomonas* enzyme was successfully overproduced in *Escherichia coli* (27, 28). This bacterial prototype of the eukaryotic SPT provided a simple model system for study-

* Corresponding author. Mailing address: Department of Biochemistry, Osaka Medical College, Takatsuki, Osaka 569-8686, Japan. Phone: 81-72-684-7291. Fax: 81-72-684-6516. E-mail for H. Ikushiro: ikushiro@art.osaka-med.ac.jp. E-mail for H. Hayashi: hayashi@art.osaka-med.ac.jp.

† Present address: Department of Biochemistry, Wake Forest University School of Medicine, Winston-Salem, NC 27157.

▽ Published ahead of print on 8 June 2007.

ing the enzyme reaction without detergent micelles or lipid membranes. However, despite the successful elucidation of the enzymological properties of the *Sphingomonas* SPT (29), we were unable to obtain crystals appropriate for a high-resolution X-ray analysis, which is essential for further clarification of the detailed catalytic mechanism of the enzyme. Therefore, we searched for SPT proteins that are suitable for crystallization in other sphingolipid-containing bacteria. One such candidate for the enzyme source is the genus *Sphingobacterium*, which is a deep-orange-pigmented rod belonging to the class *Sphingobacteria* of the phylum *Bacterioidetes* and is isolated from the environment (51) or from patients with opportunistic infections (8, 16, 23, 37, 60). *Sphingobacterium* has a high concentration of sphingophospholipids with unique branched LCBs, including ceramide phosphorylethanolamines, ceramide phosphoryl-*myo*-inositols, and ceramide phosphoryl-1-β-mannose as the major components (43, 44, 71, 72). Another candidate, *Bdellovibrio*, is a small curved rod belonging to the delta subclass of the phylum *Proteobacteria* that can be found in diverse environments, such as marine and fresh waters, sewage, and soil (47). *Bdellovibrio* is characterized by the unique predatory behavior by which it invades various other larger gram-negative bacteria and grows as a parasite in the intraperiplasmic space of the prey (46, 47, 56, 57). *Bdellovibrio* contains a phosphono ceramide, which carries the characteristic head group 1-hydroxy-2-aminoethyl phosphonate (62). The bacteria listed above are exceptions in gram-negative bacteria in that they lack lipopolysaccharides and instead contain a large amount of sphingolipids, including glycosphingolipids (33, 67–70, 72); most gram-negative bacteria contain lipopolysaccharides, the major pathogenic glycolipids of the outer membrane. glycosphingolipidss, such as α-D-glucuronosyl-ceramide and α-D-galacturonosyl-ceramide of *Sphingomonas*, were reported to activate CD1d-restricted natural killer T (NKT) cells (34, 39, 55, 66). The action of the bacterial sphingolipids in innate immunity is attracting much attention in the field of infectious diseases.

In this context, studying the SPT proteins in these bacteria is important not only for obtaining the ideal source for crystallization of the enzyme but also for providing the structural basis for the elucidation of the biosynthetic mechanism of the unique glycosphingolipids in these bacteria. We now report the molecular cloning of three novel SPTs from sphingolipid-containing bacteria, *Sphingobacterium spiritivorum* EY3101^T, *Sphingobacterium multivorum* GTC97, and *Bdellovibrio stolpii* ATCC 27052. All of these bacterial enzymes were successfully overproduced in *E. coli* and enzymatically characterized. Their properties resembled those of the eukaryotic enzyme more closely than those of the *Sphingomonas* enzyme. Thus, these enzymes can be useful models for mammalian SPT and candidates for high-resolution crystallographic analyses.

MATERIALS AND METHODS

Chemicals. L-Serine and the other natural L-amino acids were obtained from Nacalai Tesque (Kyoto, Japan). Palmitoyl CoA and lauroyl CoA were from Funakoshi (Tokyo, Japan). Isopropyl 1-thio-β-D-galactoside, myristoyl CoA, *n*-heptadecanoyl CoA, stearoyl CoA, arachidoyl CoA, palmitoleoyl CoA, and oleoyl CoA were from Sigma. The LMW gel filtration calibration kit, gel filtration calibration kit PD-10, and Sephacryl S-200 HR were from Amersham Bioscience/GE Healthcare. DEAE-Toyopearl 650 M and butyl Toyopearl 650 M were from Tosoh (Tokyo, Japan). The competent *E. coli* JM109 was purchased from Nippon Gene (Tokyo, Japan). *E. coli* BL21(DE3)(pLysS) and plasmids pET21b and pET28b were from Novagen. Plasmid pUC118 was from Takara Bio (Kyoto, Japan). All other chemicals were of the highest grade available from commercial sources.

Bacterial strains and growth conditions. *Sphingomonas paucimobilis* EY2395^T and *S. spiritivorum* EY3101^T were gifts from Eiko Yabuuchi (Gifu University School of Medicine, Gifu, Japan). *S. multivorum* GTC97 was from the Gifu Type Culture Collection of Gifu University, Japan. These three strains were aerobically grown in Bacto heart infusion broth (Difco, Becton Dickinson) at 30°C. *B. stolpii* (ATCC 27052) was purchased twice from ATCC, but it did not grow from the freeze-dried stock. A living culture was a gift from Yoko Watanabe (Niigata University, Niigata, Japan). This strain was grown in culture medium containing 1% Bacto tryptone and 0.3% Bacto yeast extract (Difco, Becton Dickinson, MD) at 30°C. The cells were collected by centrifugation and stored at −20°C before use.

Isolation and sequencing of genomic DNA clones encoding *S. multivorum* SPT. The genomic DNA of *S. multivorum* was prepared according to a standard method (5). Based on the amino acid sequences of the *Sphingomonas* SPT and eukaryotic LCB1/LCB2 proteins, we synthesized degenerate oligonucleotides to obtain partial DNA fragments encoding the *S. multivorum* SPT gene by PCR with genomic DNA from *S. multivorum*. The oligonucleotides 5′-GG(TCAG)(TA)(CG)(TCAG)TA(TC)AA(TC)TA(TC)(TA)T(AG)GG(TCAG)(TA)T-3′ and 5′-CC(TCAG)AT(TCAG)G(TA)(AG)TG(TCAG)GC(TC)TC(AG)TC-3′ corresponded to the amino acid sequences GSYNYLMGF and DEAH SMG, respectively, of the *Sphingomonas* SPT. PCR was performed using the LA *Taq* DNA polymerase (Takara Bio, Kyoto, Japan) under the following conditions: 30 cycles of 94°C for 30 s, 40°C for 30 s, and 72°C for 1 min and then 72°C for 10 min. The PCR product was directly cloned into a pCRII vector (Invitrogen) and sequenced using a DYEnamic ET Dye Terminator cycle sequencing kit (Amersham Biosciences) and an ABI 310 DNA sequencer (Perkin-Elmer). To obtain the full-length SPT gene, a genomic DNA library (3×10^4 recombinants) was screened with the ^{32}P-labeled PCR product (500 bp) as a probe. The library was constructed as follows: genomic DNA from *S. multivorum* was partially digested with Sau3AI, and fragments of between 2.5 and 3.5 kb were purified by agarose gel electrophoresis and ligated into the BamHI-digested pUC118; these constructs were used to transform the *E. coli* JM109. Labeling of the probe and detection of the hybridizing fragments were performed using the BcaBEST labeling kit (Takara Bio, Kyoto, Japan) and Quick-Hyb hybridization solution (Stratagene), respectively. Three positive clones were isolated in the first screening, and the complete DNA sequence was determined for both strands of all three clones.

Isolation and sequencing of genomic DNA clones encoding the *S. spiritivorum* SPT. Genomic DNA from *S. spiritivorum* was prepared by ISOPLANT (Wako, Osaka, Japan) according to the manufacturer's specifications. Based on the amino acid sequences of *Sphingomonas paucimobilis* and *S. multivorum* SPTs, we synthesized degenerate oligonucleotides to obtain partial DNA fragments encoding the *S. spiritivorum* SPT gene by PCR with genomic DNA from *S. spiritivorum*. The oligonucleotides, 5′-CCA(TC)GC(TCAG)TC(AG)AT(TC)(TA)(TA)(TC)GA(TC)G-3′ and 5′-CC(AG)CC(GT)A(TCAG)(TA)G(TA)(GT)(CG)C(TCAG)A(CA)CGA(TC)TT-3′, corresponded to the amino acid sequences HASIID and KSLASLGG, respectively, of the *S. multivorum* SPT. PCR was performed using the LA *Taq* DNA polymerase under the following conditions: 30 cycles of 94°C for 30 s, (40 + *t*)°C for 30 s, and 72°C for 1 min and then 72°C for 10 min, where *t* denotes that the annealing temperature was successively increased by 0.25°C for each cycle. The PCR product was cloned and sequenced. To obtain the full-length SPT gene, a genomic DNA library (4×10^4 recombinants) was screened with the ^{32}P-labeled PCR product (342 bp) as a probe. The construction of the genomic DNA library, labeling of the probe, and detection of the hybridizing fragments were carried out in the same way as for the *S. multivorum*. Two positive clones were isolated in the first screening, and the complete DNA sequences were determined for both strands of both clones.

Isolation and sequencing of genomic DNA clones encoding the *B. stolpii* SPT. Genomic DNA from *B. stolpii* was prepared by using ISOPLANT according to the manufacturer's specifications. Based on the amino acid sequences of the bacterial SPTs, we synthesized degenerate oligonucleotides to obtain partial DNA fragments encoding the *B. stolpii* SPT gene by PCR with genomic DNA from *B. stolpii*. The oligonucleotides, 5′-TGG(CA)TCACG(GT)(AT)T(CG)(TC)T(CA)AACGG(TC)AC(CG)TT-3′ and 5′-CGAC(AG)AA(GT)CC(AG)CC(GT)A(CA)TG(AT)(GT)(CG)C(GT)A(CA)CGATTTTGA-3′, corresponded to the amino acid sequences GSRFLNGTLD and SKSLASLGGFVA, respectively, of the *S. multivorum* SPT. The PCR conditions were the same as those for the *S. spiritivorum* SPT gene. To obtain the full-length SPT gene, a genomic DNA library (1×10^5 recombinants) was screened with the ^{32}P-labeled PCR product

(536 bp) as a probe. Other methods to isolate the SPT gene were the same as described above. Twenty-eight positive clones were isolated in the first screening, and the complete DNA sequences were determined for both strands of the three longest clones.

Expression of *S. multivorum*, *S. spiritivorum*, and *B. stolpii* SPT genes in *E. coli*. In order to construct an expression system for the bacterial SPTs in *E. coli*, new restriction sites, NdeI and EcoRI (for the *S. multivorum* SPT) or NdeI and SalI (for the *S. spiritivorum* and *B. stolpii* SPTs) were introduced into each SPT gene at the translation initiation and termination sites, respectively, by PCR. The internal NdeI restriction site (^{889}CATATG) of the *S. spiritivorum* SPT gene was changed to CACATG without changing the codons by site-directed mutagenesis using the QuikChange site-directed mutagenesis kit (Stratagene). Each modified DNA fragment was ligated into the pET21b or pET28a vector using the LigaFast Rapid DNA ligation system (Promega), and each recombinant plasmid was used to transform the *E. coli* BL21(DE3)(pLysS) cells. Protein expression was induced with 0.1 mM isopropyl 1-thio-β-D-galactoside and continued for 6 h at 37°C.

Purification of recombinant SPTs. All purification procedures were performed at 4°C. All buffers used for the purification contained 0.1 mM EDTA, 5 mM dithiothreitol, and 20 μM PLP unless otherwise indicated. For the purification of *B. stolpii* SPT, 20% (wt/vol) glycerol was added to the purification buffers. The cells (10 to 25 g [wet weight]) were suspended in 150 ml of 20 mM potassium phosphate buffer (pH 7.6) and disrupted by sonication (Branson Sonic Power, Sonifier model 450) at 20 kHz for 3 min, three times. The intact cells and debris were removed by centrifugation (100,000 × *g*, 60 min). The supernatant solution was applied to a DEAE-Toyopearl 650 M column (2.5 by 20 cm) equilibrated with the same buffer. The proteins were eluted with a linear gradient of 0 to 500 mM NaCl in 1 liter of 20 mM potassium phosphate. The fractions containing the SPT were collected. $(NH_4)_2SO_4$ was added to 30% saturation, and the solution was applied onto a Butyl-Toyopearl 650 M column (2.5 by 20 cm) equilibrated with the same buffer containing 30%-saturated $(NH_4)_2SO_4$. For *S. spiritivorum* SPT, the condition of 20%-saturated $(NH_4)_2SO_4$ was adapted. SPT was eluted with a decreasing linear gradient of $(NH_4)_2SO_4$ concentrations (30 to 0% or 20 to 0%) in 1 liter of 20 mM potassium phosphate. The pooled fractions were concentrated and then applied to a hydroxyapatite column (1.6 by 20 cm) equilibrated with 10 mM potassium phosphate buffer (pH 7.6). The proteins were eluted with a linear gradient of 10 to 250 mM potassium phosphate in 1 liter. The SPT fractions were concentrated and then applied to a Sephacryl S-200 HR column (1.6 by 80 cm) equilibrated with 50 mM potassium phosphate buffer (pH 7.6) containing 0.1 mM EDTA and 150 mM NaCl. The active fractions were combined, concentrated to 2 to 5 ml, filtered, and stored at 4°C.

Mass spectrometric analyses of reaction products. To identify the reaction products of the bacterial SPT, the reaction was carried out in the presence of 1.6 mg purified SPT, 20 mM L-serine, 5 mM acyl CoA, 50 mM EDTA, 50 mM HEPES, and 0.15 M KCl (pH 7.5) in a final volume of 0.1 ml. The reaction was stopped by the addition of 0.1 ml of ~2 M ammonia, and then the total lipids were extracted by the method of Bligh and Dyer (9), followed by hexane-2-propanol (3:2 [vol/vol]) and a salt solution partition (45). The lipid products were identified by electrospray ionization (ESI)/ion-trap mass spectrometry connected online to the normal-phase high-performance liquid chromatography (HPLC) (30, 58). LCBs can be analyzed by a method similar to the ceramide analysis previously reported (30), with minor modifications. A trap column (1 by 20 mm) fitted to a switching valve (Valco Instruments Co., Houston, Texas) was pre-equilibrated with solvent A (hexane containing 0.1% formic acid). An aliquot of the extracted lipids was applied onto the trap and then washed with the same solvent. Immediately after connecting the trap by valve switching to a separation silica column (1 by 150 mm; OmniSeparo-TJ, Hyogo, JAPAN) equilibrated with solvent A, the LCBs bound to the trap were eluted with the following gradient sequence: from 100% solvent A to 70% solvent A and 30% solvent B (hexane:2-propanol, 4:6 by volume) in 6 min, to 95% solvent B and 5% solvent C (hexane:2-propanol:1 M ammonium formate:water, 40:60:2.24:9.76 by volume) in 5 min, and then to 50% solvent B and 50% solvent C in 15 min. The effluent was monitored by a ThermoElectron LCQdeca mass spectrometer equipped with an ESI tip, FortisTip (20-mm inside diameter and 150-mm outside diameter; OmniSeparo-TJ, Hyogo, JAPAN) on an xyz stage (AMR, Tokyo, Japan) in positive-ion full scan and data-dependent positive-ion tandem mass spectrometry (MS/MS) modes on a single run. An ESI voltage of 1.6 kV was used.

Spectrophotometric measurements. The absorption spectra of the SPTs were recorded by a Hitachi U-3300 spectrophotometer at 25°C. The circular dichroism (CD) spectra of the SPTs were recorded by a Jasco J720-WI spectropolarimeter at 25°C. The buffer solution for the spectrometric measurements contained 50 mM HEPES-NaOH (pH 7.5), 150 mM KCl, and 0.1 mM EDTA. The purified enzyme was equilibrated with this buffer by gel filtration using a PD-10 (Sephadex G-25) column prior to the measurements.

Antibody preparation against each bacterial SPT. The antiserum against *Sphingomonas paucimobilis*, *S. multivorum*, or *B. stolpii* SPT was prepared by immunization of rabbits with the purified SPT proteins. Each anti-SPT immunoglobulin G (IgG) was affinity purified with the corresponding SPT-immobilized Sepharose 4B from the total IgG fraction of the rabbit serum by a standard method.

Immunoblot analysis. sodium dodecyl sulfate (SDS)-polyacrylamide gel electrophoresis was performed as described by Laemmli (35) with the SDS-Tris system using a 3% (wt/vol) stacking and a 10% (wt/vol) separating gel. The gels were blotted onto Immobilon-P^{SQ} polyvinylidene difluoride membranes (Millipore, MA) using a semidry blotting method. The membranes were blocked at room temperature for 2 h in phosphate-buffered saline (PBS) containing 1.5% (wt/vol) bovine serum albumin (BSA), followed by incubation with diluted anti-SPT rabbit antibodies at room temperature for 3 h. The membranes were washed and incubated with a 1:5,000 dilution of the horseradish peroxidase-conjugated goat antirabbit antibody solution at room temperature for 3 h. Visualization of the immunoreactive bands was performed using chemical luminescence (ECL detection kit; Amersham Biosciences Inc., Piscataway, NJ).

Electron microscopic analysis by the thin-section (postembedding) method. The cells were first fixed in a 0.1 M sodium cacodylate buffer (pH 7.4) containing 4% paraformaldehyde and 0.1% glutaraldehyde for 2 h at 4°C, dehydrated in a graded series of ethanol solutions (50% to 100%), and embedded in LR White resin (London Resin Co., Ltd., Hampshire, United Kingdom) overnight at 60°C. Ultrathin sections (90 nm in thickness) were prepared by an ultramicrotome (2088-V, LKB; Bromma, Sweden). The sections were transferred onto fine nickel grids and incubated in PBS containing 1% BSA and 1.5% normal goat serum for 15 min at room temperature and in PBS containing 1% BSA, 1.5% normal goat serum, and anti-SPT IgG overnight at 4°C. Subsequently, the grid was incubated in PBS containing 1% BSA, 1.5% normal goat serum, and goat anti-rabbit IgG conjugated to 10-nm gold particles for 30 min at room temperature. All sections were finally stained with uranyl acetate and lead citrate. The preparation was examined using an electron microscope, JEM2000EX (JEOL, Tokyo, Japan).

Other methods. SPT activity was measured according to previously described methods (27). The protein concentration during the purification procedure was determined using a BCA protein assay kit (Pierce Chemical) with bovine serum albumin as the standard. The protein concentration of the purified SPT was spectrophotometrically determined using the following molar extinction coefficients at 280 nm for the PLP form of each enzyme: $2.83 \times 10^4\ M^{-1} \cdot cm^{-1}$ for *S. paucimobilis* SPT (27); $2.68 \times 10^4\ M^{-1} \cdot cm^{-1}$ for *S. multivorum* SPT; $2.68 \times 10^4\ M^{-1} \cdot cm^{-1}$ for *S. spiritivorum* SPT; and $2.68 \times 10^4\ M^{-1} \cdot cm^{-1}$ for *B. stolpii* SPT.

Nucleotide sequence accession numbers. The nucleotide and protein sequences of the *spt* genes have been submitted to the GenBank database (*S. multivorum*, AB259214; *S. spiritivorum*, AB259215; *B. stolpii*, AB259216).

RESULTS

SPT activity in *S. multivorum* and *B. stolpii*. We previously reported that both *Sphingomonas paucimobilis* SPT and *S. spiritivorum* SPT are water-soluble enzymes (27). The SPT activities in *S. multivorum* and *B. stolpii* were examined in a similar way (27), and the results are presented in Fig. 1 together with those for *Sphingomonas paucimobilis*, *S. spiritivorum*, and the mouse liver microsome. For all of the bacterial strains, SPT activity was found in both the supernatant and precipitate fractions, which were prepared by ultracentrifugation. The distribution profile of the activity in the supernatant and the precipitate seems to vary depending on the species. However, since the precipitate fraction contains a nonnegligible amount of unlysed cells, it is hard to precisely estimate how much of the SPT activity is associated with the membrane. This issue was morphologically assessed using immunoelectron microscopy, as described later in detail.

Cloning of SPT genes from *S. multivorum*, *S. spiritivorum*, and *B. stolpii*. The three SPT genes (*spt*) from *S. multivorum*, *S. spiritivorum*, and *B. stolpii* were cloned by degenerate PCR and genome library screening, as described in Materials and Meth-

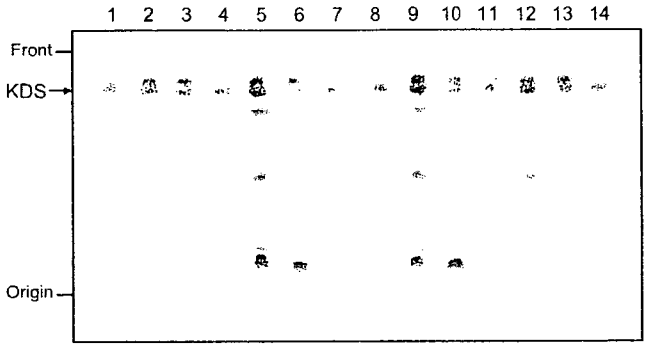

FIG. 1. Thin-layer chromatography of radiolabeled products obtained by SPT assay reactions of mouse liver microsomes, *S. paucimobilis*, *S. multivorum*, *S. spiritivorum*, and *B. stolpii*. The assay reactions and thin-layer chromatography were carried out as described in reference 27. Reaction products formed in the presence of the crude extract, the precipitate (resuspended), or the supernatant were spotted. The volume of the crude extract used for the reaction was 100 μl (140 mg protein/ml), and the amounts of the precipitate and the supernatant were those obtained from the same volume (100 μl) of the crude extract. Lanes 1 and 8, mouse liver microsomes as a reference; lanes 2, 5, 9, and 12, crude extracts after sonication of *S. paucimobilis* (lane 2), *S. multivorum* (lane 5), *S. spiritivorum* (lane 9), and *B. stolpii* (lane 12); lanes 3, 6, 10, and 13, the precipitates after centrifugation at 1,000,000 × *g* of the crude extracts of *S. paucimobilis* (lane 3), *S. multivorum* (lane 6), *S. spiritivorum* (lane 10), and *B. stolpii* (lane 13); lanes 4, 7, 11, and 14, the supernatants after centrifugation at 100,000 × *g* of the crude extracts of *S. paucimobilis* (lane 4), *S. multivorum* (lane 7), *S. spiritivorum* (lane 11), and *B. stolpii* (lane 14).

ods. Properties of the gene products of the bacterial SPTs are summarized in Table 1.

Sequence comparisons. The amino acid sequence alignment of the human SPT subunits, SPTLC1/SPTLC2/SPTLC3, products of isolated bacterial SPT genes and the putative SPT gene of *Zymomonas mobilis* ZM4 (50), and two other enzymes of the α-oxamine synthase family, i.e., *E. coli* 8-amino-7-oxononanoate synthase (AONS) and human 5-aminolevulinate synthase (ALAS), is shown in Fig. 2A. AONS and ALAS were selected as the proteins most and second most homologous to SPT, respectively. An overall sequence similarity was found between these proteins. Bacterial SPTs are highly similar to each other, and conserved amino acids are distributed throughout the entire sequences of the polypeptides. The *S. multivorum* SPT shared the highest amino acid sequence identity (87.7%) with the *S. spiritivorum* SPT. The *Z. mobilis* SPT also showed a high identity (73.1%) with the *Sphingomonas* SPT. The amino acid sequence identities among other bacterial SPTs were 35.0 to 48.2%. The conservation of the amino acid sequences between each bacterial enzyme was higher than that between the bacterial SPTs and human SPTLC proteins. *S. multivorum* SPT is 25%, 31%, and 32% identical, *S. spiritivorum* SPT is 27%, 32%, and 33% identical, and *B. stolpii* SPT is 24%, 33%, and 34% identical to human SPTLC1, SPTLC2, and SPTLC3, respectively. Several small hydrophobic stretches of amino acids were distributed throughout the bacterial SPT protein; however, no obvious transmembrane region(s) were found. The SPT-specific PLP-binding motif (GTFSKSXXXXGG) is completely conserved among all the bacterial SPTs.

A phylogenetic tree of the SPTs was constructed by the neighbor-joining method using the *E. coli* AONS protein as an outgroup (Fig. 2B). The selection of this protein as the outgroup was done because *E. coli* AONS is the protein apparently distinct from SPT but has the highest similarity to SPT among the α-oxamine synthase family enzymes. The bootstrap values at the nodes, except for the leftmost two nodes, were all 100%. The reason for the relatively low values of 74% and 82% of the two nodes is not clear, but it may be partially attributed to the use of the evolutionarily distant (i.e., functionally different) outgroup. The divergence of the bacterial SPTs reflects the phylogeny of the bacteria; *Sphingomonas paucimobilis* and *Z. mobilis* belong to the same family of bacteria, called *Sphingomonadaceae*, and *S. multivorum* and *S. spiritivorum* belong to the family *Sphingobacteriaceae* (50, 69). The branch lengths of the LCB1 proteins are significantly greater than those of other proteins, including the LCB2, SPTLC3, and bacterial SPTs, suggesting relatively higher evolution rates of the LCB1 proteins. *S. spiritivorum* SPT is the nearest relative to the mammalian LCB2 proteins, followed by the SPTs from *S. multivorum*, *B. stolpii*, *Z. mobilis*, and *Sphingomonas paucimobilis*.

Overproduction and purification of recombinant SPTs. Each bacterial SPT has been stably overexpressed as a soluble protein in *E. coli*. The expression levels of the recombinant proteins reached approximately 10 to 20% of the total protein of *E. coli* cells without growth inhibition of the expression host. While the *B. stolpii* SPT was most abundantly expressed, half of the expressed protein formed inclusion bodies. In order to increase the solubility of the recombinant enzyme, we made a deletion variant of the *B. stolpii* SPT lacking the N-terminal 13 amino acid residues. The addition of 20% (wt/vol) glycerol was necessary to prevent the precipitation of the *B. stolpii* SPT during purification and storage. All of the recombinant enzymes were purified to homogeneity by column chromatography in three steps, and the purified SPTs showed a single protein band with an apparent M_r of approximately 45,000 for the *S. multivorum* and *S. spiritivorum* SPTs and 50,000 for the *B. stolpii* SPT, respectively, by SDS-polyacrylamide gel electrophoresis (data not shown). About 20 mg of purified enzyme was routinely obtained from 1-liter cultures in each case and could be stored at 4°C for more than 6 months.

Physicochemical characterizations. The M_r values of all three bacterial SPTs were estimated to be 90,000 by gel filtration. Matrix-assisted laser desorption ionization–time-of-flight MS analyses gave a signal at *m/z* 43,645 for the *S. multivorum* SPT, 43,780 for the *S. spiritivorum* SPT, and 44,397 for the *B. stolpii* SPT lacking the N-terminal 13 amino acid residues. These values were in good agreement with the values of 43,640, 43,797 and 44,522, which were calculated from the deduced amino acid sequences of each recombinant enzyme without the first methionine within experimental error. These results show

TABLE 1. Bacterial SPTs

Bacterial species	GenBank accession no. of SPT	ORF size (bp)[a]	[G+C] (%)	M_r	pI
S. paucimobilis	AB055142	1,263	65.00	45,041	5.66
S. multivorum	AB259214	1,200	38.33	43,771	5.05
S. spiritivorum	AB259215	1,200	41.08	43,929	4.97
B. stolpii	AB259216	1,263	43.31	46,172	6.25

[a] ORF, open reading frame.

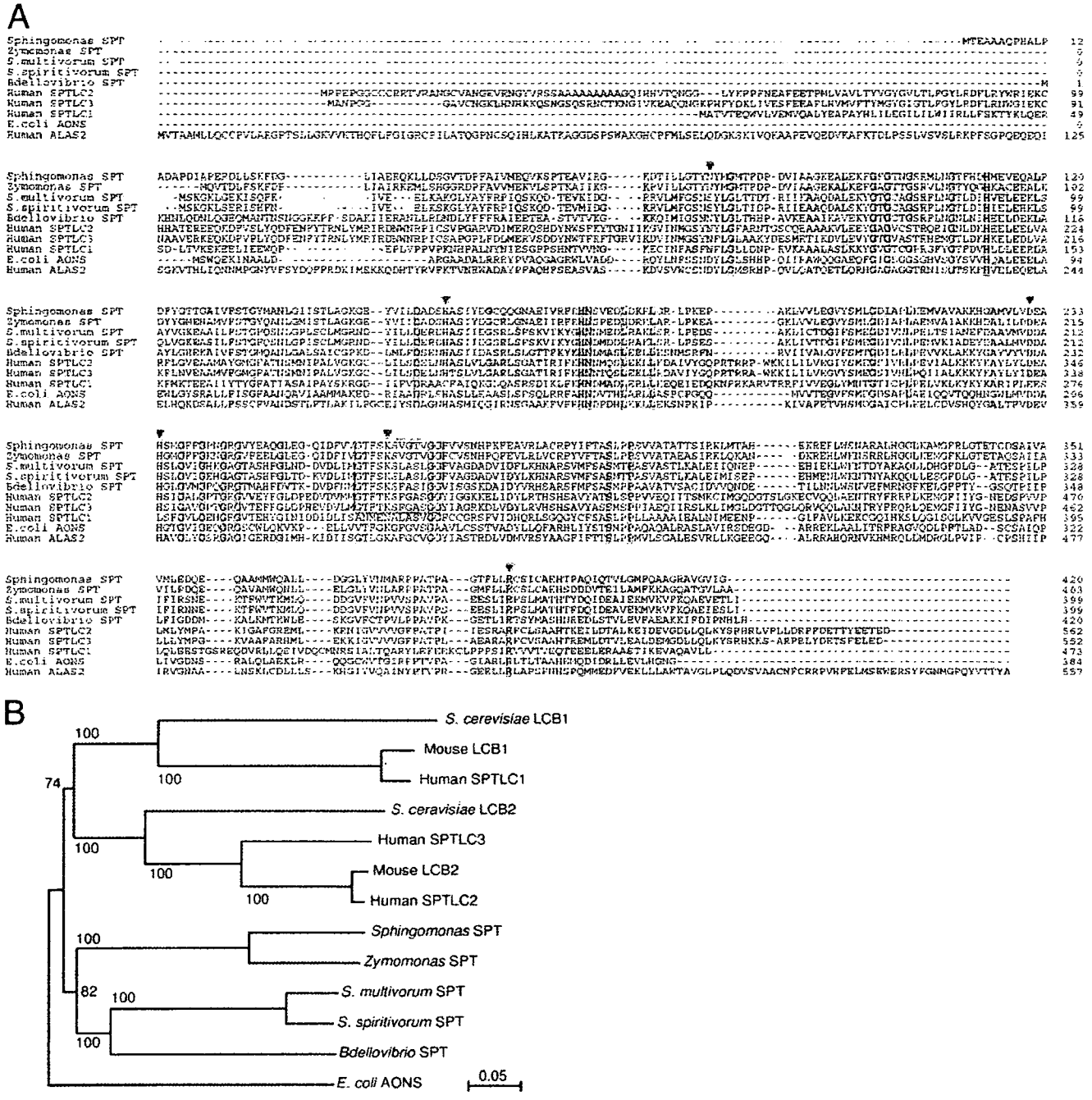

FIG. 2. Sequence alignment and molecular phylogenetic tree of SPTs. (A) Aligned sequences of bacterial SPTs, human SPT subunits (SPTLC1, SPTLC2, and SPTLC3), *E. coli* AONS, and human ALAS2. The deduced amino acid sequences of the SPTs and other proteins were aligned using the CLUSTALX version 1.83 program (59). The gap opening and extension parameters were set to 10 and 0.2, respectively. Zymomonas SPT, *Zymomonas mobilis* SPT; Sphingomonas SPT, *Sphingomonas paucimobilis* SPT; S. multivorum SPT, *Sphingobacterium multivorum* SPT; S. spiritivorum SPT, *Sphingobacterium spiritivorum* SPT; Bdellovibrio SPT, *Bdellovibrio stolpii* SPT. Residues identical among all the proteins are in light blue, and those conservatively substituted are in green. Residues indicated by the reverse triangle are active-site residues that are considered to be important for catalysis. The red-boxed sequences are the SPT-specific PLP-binding motif (GTFSKSXXXXGG). (B) Molecular phylogenetic tree of SPTs from various sources. The phylogenetic tree was constructed by the neighbor-joining method using the *E. coli* AONS protein as an outgroup. The number at each node represents the bootstrap value as a percentage of 1,000 replications.

that these bacterial SPTs have dimeric structures composed of two identical subunits.

The pH stability of the purified SPTs was investigated (data not shown). This information is necessary for both crystallization and storage. Enzymes from both *S. spiritivorum* and *B. stolpii* SPTs showed an above-90% activity in the pH range of 6.8 to 8.5, with an optimum pH at 7.0 to 8.0. Only the *S. multivorum* SPT was denatured below pH 7.2, and its optimum pH was 7.4 to 8.0.

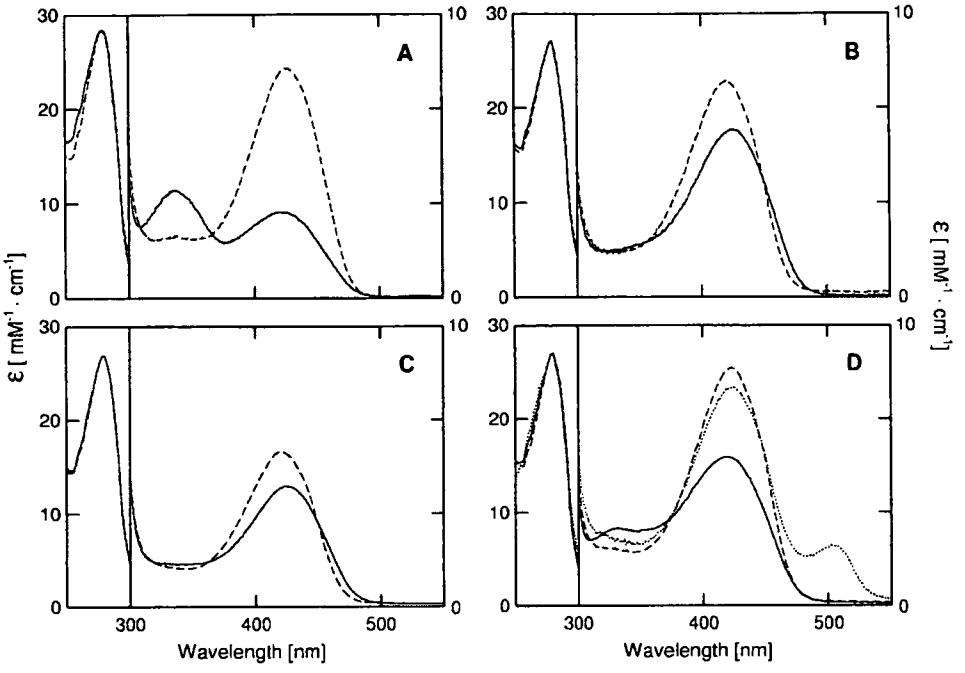

FIG. 3. Absorption spectra of purified SPTs. The purified SPTs (10 μM) were dissolved in 50 mM HEPES-NaOH (pH 7.5) containing 150 mM KCl and 0.1 mM EDTA, and their absorption spectra were measured at 25°C. (A to C) Absorption spectra of the *Sphingomonas paucimobilis*, *S. multivorum*, and *S. spiritivorum* SPTs in the absence (solid line) or presence (dashed line) of 45 mM L-serine. (D) Absorption spectra of the *B. stolpii* SPT in the absence (solid line) or presence (dashed line) of 100 mM L-serine. The dotted line shows the spectrum in the presence of 100 mM L-serine and 90 μM palmitoyl CoA.

All purified recombinant SPTs showed characteristic absorption spectra of PLP-dependent enzymes (Fig. 3). For all of the bacterial SPTs, the intensities of the absorption peaks were not changed by the pH. The shapes of the spectra of the two *Sphingobacterium* SPTs were different from that of the *Sphingomonas* enzyme (Fig. 3A, B, and C). They had only a single peak at 426 nm in addition to the protein absorption peak at 278 nm. On the other hand, the *B. stolpii* SPT showed two peaks, at 338 and 426 nm (Fig. 3D), and in this respect was similar to the *Sphingomonas* enzyme, although the relative intensities of the two peaks are different. These absorption peaks, respectively, correspond to the enolimine and ketoenamine forms of the internal Schiff base (aldimine formed between the aldehyde group of PLP and the ε-amino group of a lysine residue in the active site) of SPT. The addition of L-serine to the purified SPTs gave rise to an intense absorption band at 426 nm for all of the SPTs and a weak band at 338 nm for the *Sphingomonas* and *B. stolpii* SPTs. These spectral changes showed hyperbolic dependencies on the concentrations of L-serine, and the apparent dissociation constants (K_D) for L-serine were calculated to be 0.47, 1.20, and 2.55 mM, respectively, for the *S. multivorum*, *S. spiritivorum*, and *B. stolpii* SPTs (Table 2). The CD spectra of these bacterial SPTs showed positive bands at 426 nm (and additionally at 338 nm for *B. stolpii* SPT), corresponding to the absorption spectra of each enzyme (data not shown). The CD spectra in the presence of a saturating amount of L-serine showed a negative band at 426 nm (data not shown). These results indicate that the added L-serine formed the external Schiff base (aldimine formed between PLP and extraneously added amino acid) with PLP. The addition of the second substrate, palmitoyl CoA, to the *B. stolpii* SPT, which is saturated with L-serine, resulted in a slight decrease in the 426-nm peak and the appearance of an absorption band at 515 nm (Fig. 3C). The formation of the 515-nm peak was transient, and the peak vanished within a few minutes. Such spectral changes were not observed for the *Sphingobacterium* SPTs or the *Sphingomonas* SPT.

Identification of reaction products of bacterial SPTs. The formation of KDS by bacterial enzymes was confirmed by HPLC/ESI–ion-trap mass spectrometry (Fig. 4). Figure 4A shows the ion chromatograms (*m/z* 300) of the SPT reaction product in the positive-ion mode. The most abundant ions at *m/z* 300 (Fig. 4C) corresponded to the protonated molecular ions $[M + H]^+$ of C18:0 KDS formed from L-serine and palmitoyl CoA, the structure of which is shown in Fig. 4B. This LCB

TABLE 2. Kinetic parameters of bacterial SPTs

Bacterial species	Value for SPT parameter			
	K_D (Ser) (mM)	K_m (Ser) (mM)	K_m (palmitoyl CoA) (mM)	k_{cat} (s^{-1})
S. paucimobilis	1.40 ± 0.10	4.7 ± 0.6	0.69 ± 0.09	2.3 ± 0.11
S. multivorum	0.47 ± 0.10	4.8 ± 0.6	0.10 ± 0.01	0.12 ± 0.01
S. spiritivorum	1.20 ± 0.03	5.0 ± 0.8	0.39 ± 0.04	0.15 ± 0.01
B. stolpii	2.55 ± 0.12	3.7 ± 0.4	ND[a]	0.03 ± 0.002[b]

[a] ND, not determined.
[b] $v/[E_t]$ value in the presence of 100 μM of palmitoyl CoA.

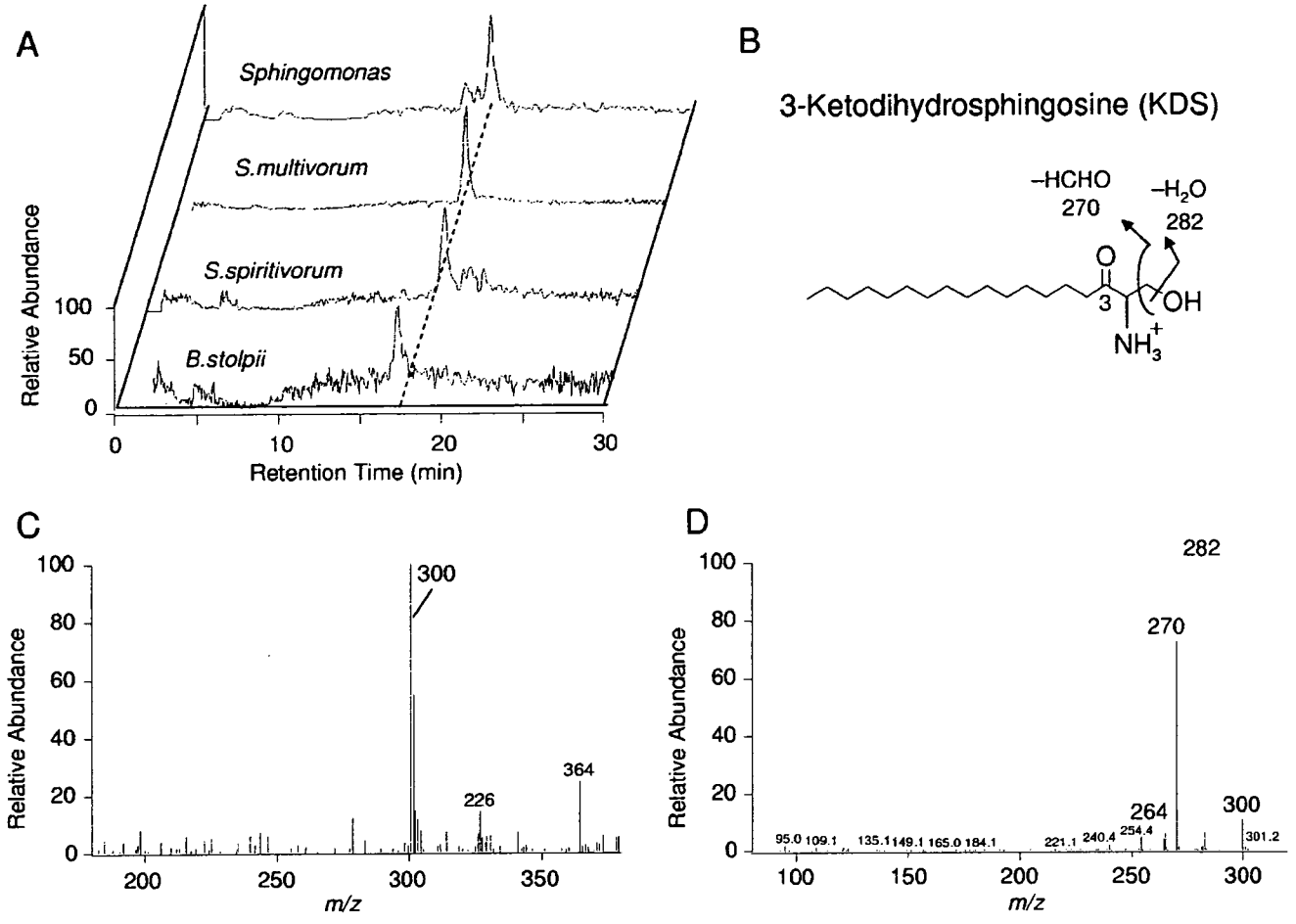

FIG. 4. HPLC/ESI-ion-trap mass spectroscopy of reaction products of bacterial SPTs. (A) Ion chromatography of the reaction products of bacterial SPTs. (B) The structure of KDS, position of fragmentation, and the size of the fragment ion are indicated. (C) MS data for the reaction product of the *S. multivorum* SPT. (D) MS-MS data for the reaction product of the *S. multivorum* SPT.

structure was confirmed by on-line MS/MS. A positive-ion MS/MS spectrum of the *m/z*-300 ion showed the presence of ions of *m/z* 282 and 270, arising from the neutral loss of H_2O and HCHO, respectively (Fig. 4B and D).

Catalytic properties of bacterial SPTs. Like eukaryotic enzymes, all of the bacterial SPTs used only the L configuration of serine as an amino acid substrate. The bacterial enzymes exhibited a broad substrate specificity concerning the chain length and the degree of unsaturation of acyl CoA (Fig. 5). Figure 5A shows ion chromatograms of the reaction product formed by the *S. multivorum* SPT. In each chromatogram, a single ion peak of the reaction product with a molecular weight corresponding to the value expected from the chain length of the acyl CoAs was detected. The longer chain length of KDS gave a slightly shorter retention time. Figure 5B shows the MS data in which the molecular ion at *m/z* 356 corresponded to $[M + H]^+$ of C22:0 KDS formed from L-serine and arachidoyl CoA. As shown in Fig. 5C, the MS/MS spectrum of the *m/z*-356 ion indicated the presence of ions of *m/z* 338, 326, and 320, arising from the neutral loss of H_2O, HCHO, and $2H_2O$, respectively. The structures of the other KDS with different chain lengths were also confirmed in the same way.

Figure 6 shows the substrate concentration dependency of the reaction rate of the bacterial SPTs. It has been reported that eukaryotic SPT is inhibited by palmitoyl CoA concentrations greater than 50 μM (20, 53). A similar phenomenon was observed with the *B. stolpii* SPT, which was significantly inhibited by palmitoyl CoA concentrations greater than 100 μM (Fig. 6C). The SPTs of *S. multivorum* and *S. spiritivorum* were not inhibited by the high concentrations of palmitoyl CoA. For the last two enzymes, we could analyze the experimental data under steady-state conditions according to the ordered Bi-Bi mechanism (Fig. 6A and B) (49), and the kinetic parameters were obtained (Table 2). For all the enzymes, the K_m values for L-serine were in the range of 3 to 5 mM. The k_{cat} values of the *S. multivorum* and *S. spiritivorum* enzymes are apparently lower than that of the *S. paucimobilis* enzyme. The K_m values for palmitoyl CoA were 0.1 to 0.7 mM, except for the *B. stolpii* enzyme. For the *B. stolpii* enzyme, the K_m value for palmitoyl CoA and k_{cat} value could not be obtained due to the substrate inhibition by palmitoyl CoA. For comparison with other data, the $v/[E_t]$ value in the presence of 100 μM palmitoyl CoA, where the maximum activity is obtained, is shown.

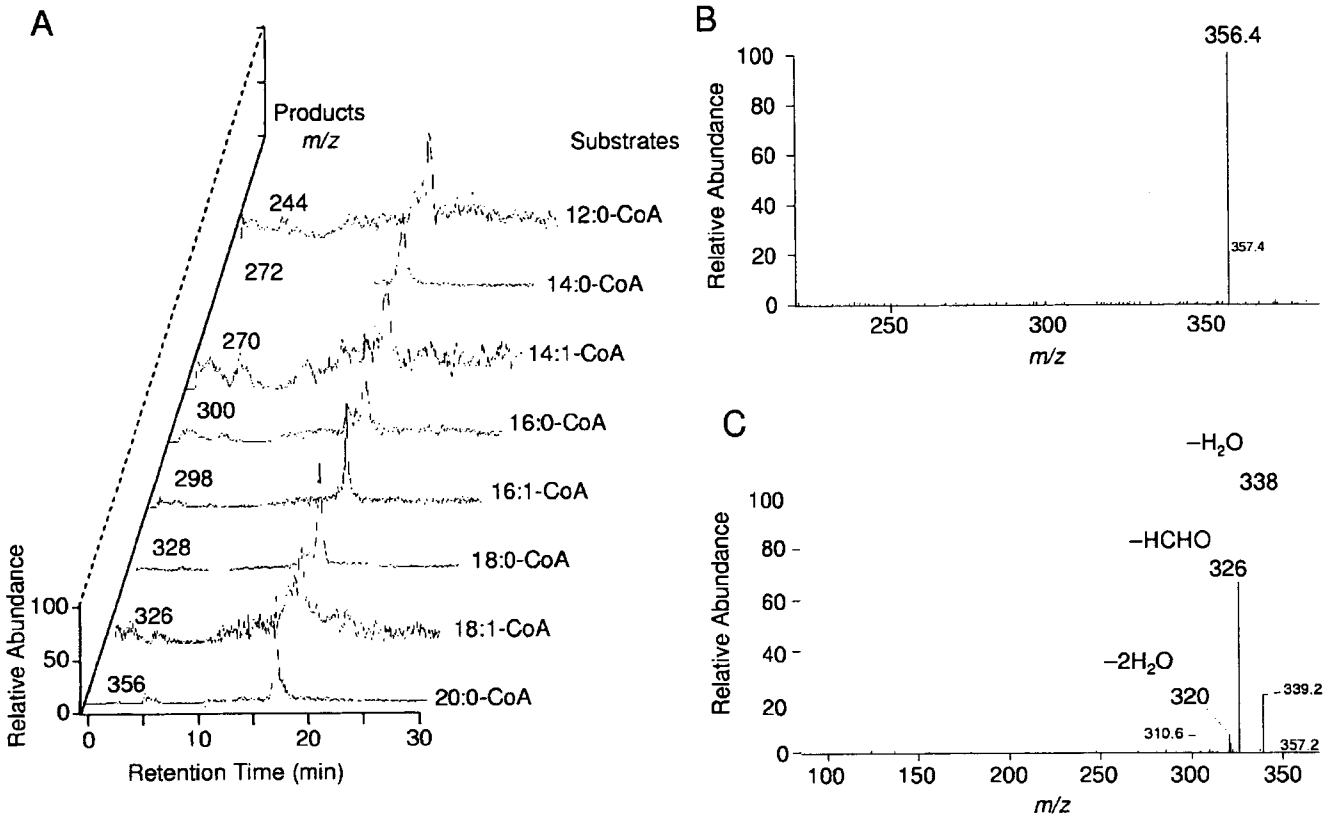

FIG. 5. HPLC/ESI-ion-trap mass spectroscopy of reaction products with various chain lengths formed by the *S. multivorum* SPT. (A) Ion chromatography of the reaction products with various chain lengths formed by the *S. multivorum* SPT. (B) MS data for the reaction product of the *S. multivorum* SPT from L-serine and arachidoyl CoA (C20:0). (D) MS-MS data for the reaction product of the *S. multivorum* SPT from L-serine and arachidoyl CoA (C20:0).

Intracellular localization of bacterial SPTs (immunolocalization). In order to examine the localization of the SPTs in the intact cell, specific polyclonal antibodies were prepared using the recombinant enzymes. As shown in Fig. 7, each antibody specifically recognized its corresponding SPT. There was no signal in the lanes containing the *E. coli* lysate transformed with the empty vector (Fig. 7, lanes 1, 4, and 7). The anti-*S. multivorum* SPT antibody cross-reacted with the *S. spiritivorum* SPT (data not shown). Considering the phylogenetic similarity of *S. spiritivorum* to *S. multivorum*, which might yield similar morphological results, and the technical constraints on the morphological analysis of this weak pathogenic species, *S. spiritivorum* was excluded from further analyses. For the *B. stolpii* lysate, the antibody recognized two bands, of approximately 50 kDa and 48 kDa, the latter being the same size as the recombinant SPT lacking the N-terminal 13 amino acid residues (Fig. 7, lanes 8 and 9). The thin sectioned profiles of the whole bacterial cells of *Sphingomonas paucimobilis*, *S. multivorum*, and *B. stolpii* are presented in Fig. 8A, B, and C, respectively. *Sphingomonas paucimobilis* cells have a rod shape, and the average size (width) of the cells was 0.8 μm (Fig. 8A). The cytoplasm of the *Sphingomonas paucimobilis* cells was characterized by the presence of clearly identifiable ribosome particles and a nonnucleoid electron-dense area. The cell envelope consisted of a one-electron-dense bilayer as an outer membrane and one additional bilayer structure as an inner membrane. The ribosome particles showed a condensed distribution near the inner membrane or the nonnucleoid electron-dense area. The shape of the *S. multivorum* cells was also rod type, and the average size (width) was 0.45 μm (Fig. 8B). The *S. multivorum* cells were slightly shorter than the *Sphingomonas paucimobilis* cells and had no flagella. At the inside of the cell wall, a multilayered inner membrane structure was observed. The *B. stolpii* cells had the shape of curved rods or spheres with a rugged cell wall (Fig. 8C). The average size (width) of the cells was 0.36 μm. As with *Sphingomonas paucimobilis* and *S. multivorum*, a multilayered cell membrane structure was seen inside of the cell wall of the *B. stolpii* cells. The ribosome particles were widely distributed in the electron-dense cytoplasm. In the middle of the cytoplasm, an organelle-like multilayered membrane structure was observed. The intracellular localization of SPT was analyzed for each bacterium using immunoelectron microscopy. The immunogold-labeled SPT was readily detectable as a spot-like distribution throughout the cytoplasm in the *Sphingomonas paucimobilis* cells (Fig. 8D). The nonnucleoid electron-dense area observed in these bacterial cells was more intensely immunostained. Some of the immunogold clusters seemed to localize near the inner membrane of the cell. Sparse immunogold particles were also detected on the outside of the cell. In the *S. multivorum* cells, about 88% of the immunogold-labeled SPT was distributed near the inner membrane of the cell, and the remaining im-

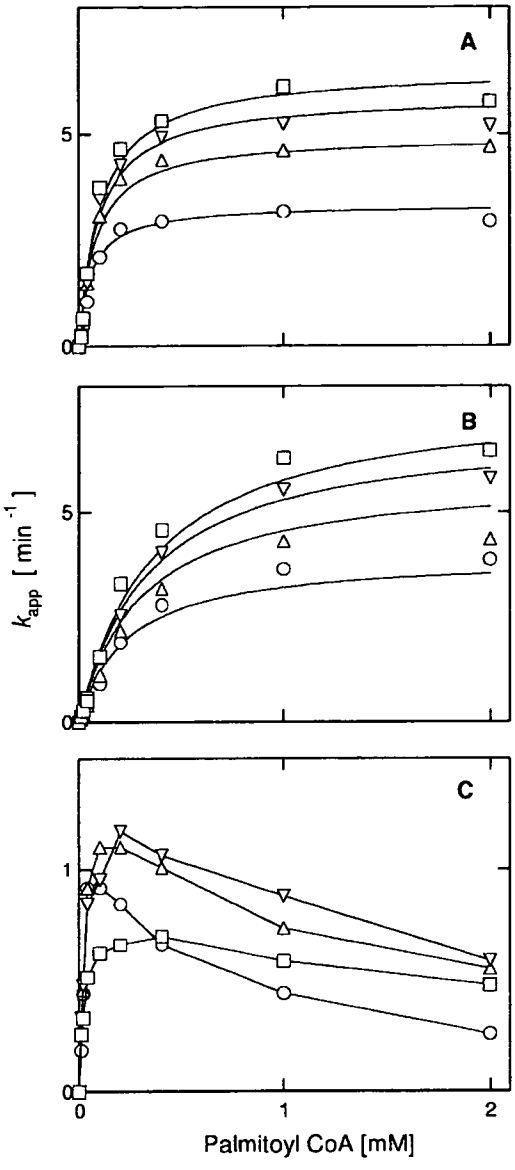

FIG. 6. Kinetic characterization of recombinant SPTs. The enzyme assay was performed as previously described (27). The apparent rate constants ($k_{app} = v/[E_t]$) for the KDS formation were plotted as a function of the palmitoyl CoA concentration at fixed concentrations of serine: 4 mM (open circle), 10 mM (open triangle), 20 mM (inverted open triangle), or 40 mM (open square). Each solid line represents the theoretical curve according to the initial velocity kinetics for the ordered Bi-Bi mechanism using the kinetic parameters summarized in Table 2. (A) *S. multivorum* SPT; (B) *S. spiritivorum* SPT; (C) *B. stolpii* SPT.

munogold particles were detected in the center of the cell (cytoplasm) (Fig. 8E). In the *B. stolpii* cells, the immunogold-labeled SPT was detected in a spot-like pattern predominantly concentrated in a limited region near the inner membrane or organelle-like multilayered membrane structure (Fig. 8F). When each primary antibody had been preabsorbed with the corresponding SPT protein, the signals disappeared or at least became very faint (Fig. 8G to I).

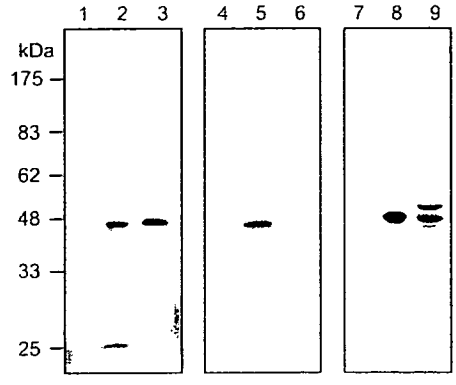

FIG. 7. Specificities of anti-SPT antibodies. The specificities of the antibodies against each bacterial SPT were confirmed by Western blot analysis with cell lysates: lanes 1, 4, and 7, *E. coli* BL21(DE3)(pLysS)(pET21) (empty vector); lane 2, *E. coli* BL21(DE3)(pLysS)(pET21-aSPT) (expressing the *Sphingomonas* SPT); lane 3, *Sphingomonas paucimobilis*; lane 5, *E. coli* BL21(DE3)(pLysS)(pET21-bSPT) (expressing the *S. multivorum SPT*); lane 6, *S. multivorum*; lane 8, *E. coli* BL21(DE3)(pLysS)(pET21-dSPT) (expressing the *B. stolpii* SPT); lane 9, *B. stolpii*.

DISCUSSION

Our recent efforts to crystallize SPT using the recombinant enzyme from *Sphingomonas paucimobilis*, which we had previously characterized, showed that the stability of the *Sphingomonas* SPT was not sufficient for crystallization and structural analysis. To obtain a suitable protein for crystallization, we searched for SPTs from other bacterial sources. *S. multivorum*, *S. spiritivorum*, and *B. stolpii* have been reported to contain large amounts of sphingolipids as cell membrane components (47, 62). Their SPT activities in the cytosolic fractions were comparable to that of *Sphingomonas paucimobilis*. Based on the amino acid sequences of the conserved regions between *Sphingomonas* SPT and the eukaryotic LCB1/LCB2 proteins, we carried out degenerate PCR and genomic library screening. Three novel SPT genes were isolated from these bacteria. Each recombinant protein catalyzed the KDS formation from L-serine and palmitoyl CoA (Fig. 4), confirming that the products of all of the cloned genes have SPT activity.

Catalytically important amino acid residues are conserved in bacterial SPTs. SPT belongs to the α-oxamine synthase family of the PLP-dependent enzymes, which includes ALAS, 2-amino-3-ketobutyrate ligase (KBL), and AONS (1, 2, 4, 32, 48, 63). Bacterial SPTs show about a 30% identity with other members of this family. Previous X-ray crystallography on AONS and KBL from *E. coli* suggested catalytically important active-site residues that interact with PLP and are completely conserved in all of the bacterial SPTs. These conserved residues include (in *S. multivorum* numbering) Lys244, which forms a Schiff base linkage with PLP, Asp210, which forms a salt bridge/hydrogen bond with the pyridine N of PLP, His213, which hydrogen bonds to 3-O of PLP, and His138, which stacks with the pyridine ring of PLP (Fig. 2A). The structures of the complexes of AONS and KBL with substrate analogues suggested that Asn52 and Arg367 are the potential hydrogen-bonding partners of the carboxylate group of the substrate L-serine in the external aldimine complex of SPT. Arg367 is indeed conserved in all of the SPTs, but Asn52 is partially

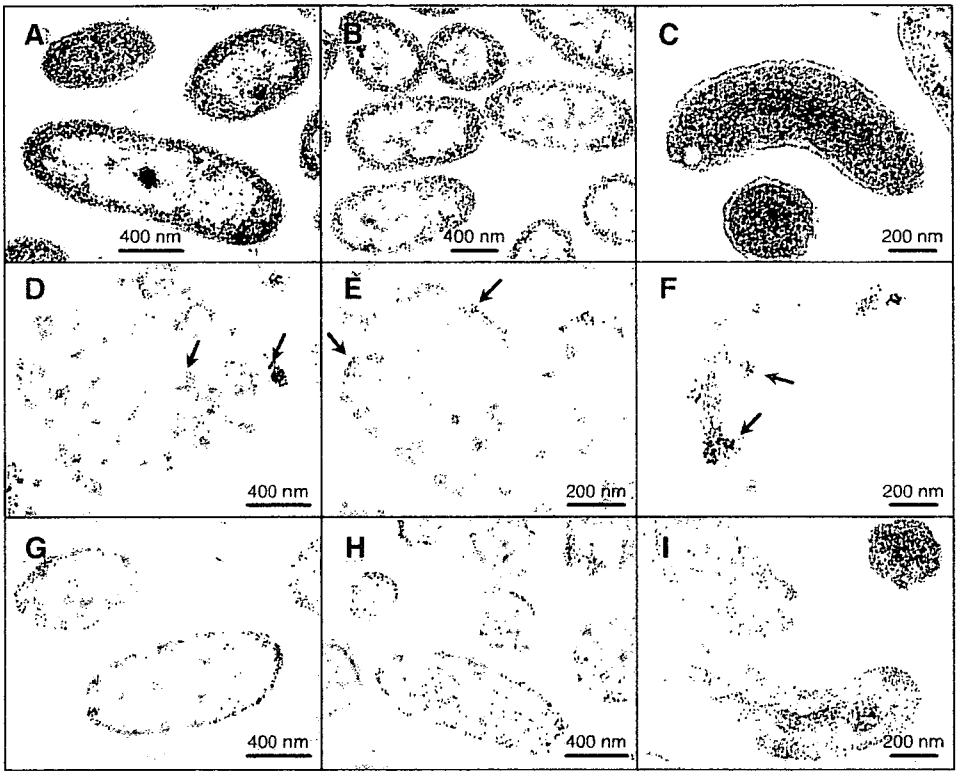

FIG. 8. Electron microscopy of sphingolipid-containing bacteria. Upper panels, morphological examination of sphingolipid-containing bacteria. Ultrathin sections of the bacterial cells were negatively stained and examined by electron microscopy. (A) *Sphingomonas paucimobilis*; (B) *S. multivorum*; (C) *B. stolpii*. Middle panels, the intracellular localization of SPT. The localization of SPT was analyzed by the postembedding immunogold-labeling method of electron microscopy. Ultrathin sections of bacterial cells were treated with anti-SPT antibody and stained with gold-labeled secondary antibodies. (D) *Sphingomonas paucimobilis*; (E) *S. multivorum*; (F) *B. stolpii*. Arrows indicate the condensed distribution of immunogold particles. Lower panels, the negative control section. Ultrathin sections of bacterial cells were treated with a preabsorbed primary antibody solution and stained with gold-labeled secondary antibodies. An excess of the purified SPT protein was added to the primary antibody working solution, and the solution was incubated at 4°C for 48 h before it was added to each section. (G) *Sphingomonas paucimobilis*; (H) *S. multivorum*; (I) *B. stolpii*. Size markers are indicated.

conserved; it shifts by one residue in the *Sphingomonas* and *Z. mobilis* SPTs.

The sequence similarities between the bacterial SPTs and human LCB2 are higher than those between the bacterial enzymes and human LCB1. The active-site residues described above are not conserved in the human LCB1; Lys244, His213, and His138 are replaced by Asn, Leu, and Cys, respectively. These residues in LCB1 cannot functionally substitute for the corresponding residues of the other α-oxamine family enzymes, including LCB2. Apparently, LCB1 does not have a catalytic function. This is consistent with the longer branch length of LCB1, because the lack of functional constraints on the protein is considered to accelerate the evolution rate.

Human hereditary sensory neuropathy type I-related mutation site of bacterial SPT. The single mutations (C133Y, C133W, V144D, or G387A) in human LCB1 cause HSN1, which is the most common hereditary disorder of peripheral sensory neurons (6, 11, 61). It remains elusive how the LCB1 mutations cause changes in the SPT activity of the heterodimer and how these changes participate in the neurodegenerative symptoms in HSN1. The dominant-negative inhibition of the SPT activities by overexpression of the HSN1-related LCB1 mutants in yeast, CHO cells, and transgenic mouse strongly supports the idea that the neurodegeneration in HSN1 is related to a decrease in the sphingolipid synthesis (7, 17, 40). However, there is a claim that the remaining SPT activity is sufficient for the normal sphingolipid metabolism and viability of the HSN1 patient cells (12). An alternative mechanism is that the HSN1 mutations of LCB1 accelerate the aggregation of the SPT protein induced by hypoxia in the human lymphocytes, which leads to nonapoptotic death (13). Contrary to these observations, de novo glucosyl ceramide synthesis increased in the lymphoblast cell lines from HSN1 patients (11), suggesting that the neural degeneration in HSN1 is due to the overproduced ceramide or the abnormal cellular lipid composition. Cys133 and Val144 of human LCB1 correspond to Cys78 and Ile90, respectively, of *S. multivorum* SPT. These residues are also conserved in the SPTs of *S. spiritivorum* and *B. stolpii* but not in *Sphingomonas paucimobilis* and *Z. mobilis* sequences, in which Cys133 and Val144 correspond to Thr and Asp/Gly, respectively. It should be noted that *Sphingomonas* SPT, which carries an amino acid substitution equivalent to the HSN1-type mutation (Asp at the position of Val144 in human Lcb1p), has a much higher activity than other bacterial enzymes carrying a hydrophobic amino acid (Ile) at that position. These findings lead us to speculate on the possibility that the

HSN1-type mutations in human LCB1 may result in some toxic gain of function, such as increased activity toward normal or abnormal acyl CoAs.

Immunolocalization of bacterial SPT as a peripheral membrane protein. All of the bacterial SPTs examined so far are water-soluble homodimeric enzymes. Their water-soluble character is the most different aspect in relation to the membrane-bound enzymes of the eukaryotes. The reaction product of SPT, KDS, is a very hydrophobic sphingolipid intermediate that is easily incorporated into membranes. While membrane localization of the eukaryotic SPT complex seems very reasonable, the characteristics of the bacterial SPT as a water-soluble protein in vitro raised questions about the mechanism of the product release or the interaction with the cellular membrane in vivo. Therefore, we further analyzed the intracellular localization of the bacterial SPT by immunoelectron microscopy (Fig. 8). These results demonstrated the limited distribution of SPT molecules in bacterial cells in a spot-like pattern (*Sphingomonas paucimobilis*) or a clearly condensed pattern near the inner membrane of the cells (*S. multivorum* and *B. stolpii*). These results are different from the homogenous distribution pattern of the general soluble proteins. *S. multivorum* and *B. stolpii* SPT may loosely bind to the inner membrane of bacterial cells like a peripheral membrane protein or may indirectly interact with the membrane via some anchor protein in vivo. The KDS released from these SPTs may directly enter the inner membrane and then be efficiently converted into various glycosphingolipids as the final products by other modification enzymes, which may be present in the bacterial cell membrane.

Most eukaryotic-like SPT from *B. stolpii*. The SPT from *B. stolpii* is different from the other bacterial SPTs in the following ways. First, during purification, the recombinant enzyme required the addition of 20% glycerol, which is the most general stabilizer for membrane proteins. Second, *B. stolpii* has an organelle-like multilayered membrane structure within the cell, and the immunoreaction to the native SPT was detected on the cytosolic face of the organelle-like structure. Third, the reaction rate is the lowest among the bacterial SPTs examined and is on the same order as the eukaryotic enzymes. Fourth, when both L-serine and palmitoyl CoA were added to the enzyme, a transient accumulation of the quinonoid intermediate was spectroscopically detected, suggesting a slow catalytic turnover of the enzyme. Finally, inhibition by palmitoyl CoA as seen in the mammalian SPTs was observed. These data indicate that the *B. stolpii* SPT is the most eukaryotic-like enzyme among the bacterial STPs, although it is a bacterial homodimeric SPT and in this respect different from the heterodimeric enzymes of the eukaryotes.

The physiological function of the sphingolipids in bacteria is unknown except for their role as a main component of the bacterial cell membrane. The broad acyl CoA specificity of bacterial SPT might be advantageous to bacteria in that they can escape from the influence of the environmental changes on bacterial envelope properties that affect their survival. If the fatty acids available to the bacterial cells are changed, their SPTs can utilize other acyl CoAs with different chain lengths for LCB synthesis. On the other hand, there is no current report that these organisms produce sphingolipids of various LCB lengths depending on the substrate fatty acids to which they are exposed. Considering that the ^{14}C-labeled palmitic acid in the culture medium is selectively incorporated into the LCB of *Sphingomonas* under normal conditions (70), it seems more probable that these organisms make essentially the same sphingolipid LCBs regardless of the fatty acid composition in the environment. This is a future research topic.

There is an interesting report demonstrating that the predatory bacterium *Bdellovibrio bacteriovorus* UKi2 contains phosphosphingolipids, and the mutant strain UKi1, lacking sphingolipids, loses its parasitic ability (56). The sphingolipids of *Bdellovibrio* may be associated in some way with the ability of this bacterium to attack and grow on suitable bacterial hosts. It has been reported that the glycosphingolipids from *Sphingomonas* sp. and *Ehrlichia muris* were recognized by the CD1d-restricted NKT cells in the mouse and human, which provide an innate-type immune response (34, 39, 55, 66). We have found putative SPT genes among the genome databases of some pathogenic bacteria and have already examined the SPT activities of these gene products. These pathogenic bacteria may also have cell walls containing glycosphingolipids that serve as direct targets for the NKT cells. Another example of the possible involvement of sphingolipids in pathogenesis is shown by a recent finding that the marine planktonic pathogen *Coccolithovirus* EhV-86 has a cluster of genes highly homologous to the enzymes of the sphingolipid metabolism (65) and these genes are coordinately expressed within 2 h of infection (3). This viral SPT is a unique monomeric enzyme, which is composed of two separable domains, suggesting a fused heterodimer corresponding to the eukaryotic SPTs (18). This viral SPT expressed in the yeast cell was localized to the endoplasmic reticulum and preferred myristoyl CoA (C14) to palmitoyl CoA (C16) as the substrate. It was suggested that the viral SPT may alter the sphingolipid metabolism of the host during pathogen infection.

We obtained novel SPT molecules with various characteristics, from the highly stable and water-soluble type to the eukaryotic-like and loosely membrane-bound type. Recently the recombinant SPT from *S. multivorum* yielded crystals of sufficiently good quality for X-ray crystallographic analysis. Further structural analyses of the SPT complex with the substrate, product, or analogues are now under way. Not only the *S. multivorum* SPT but also other bacterial enzymes will be useful because they have the characteristic spectroscopic features reflecting the intermediate accumulation of each step in the catalytic cycle. The reaction mechanism of SPT could be clarified in the context of the three-dimensional structure of the bacterial SPT. Information obtained from the bacterial enzymes will provide clues to the reaction mechanism of the more complex eukaryotic homologue.

ACKNOWLEDGMENTS

We thank Eiko Yabuichi of Aichi Medical University, Yoshiaki Kawamura of Aichi Gakuin University, and Yoko Watanabe of Niigata University for generously providing bacterial strains. We also acknowledge Nobuyoshi Esaki and Tatsuo Kurihara of Kyoto University for useful comments on the immunoelecromicroscopic study.

This work was supported by a Grant-in-Aid for Encouragement of Young Scientists (B), 16770103, and a Grant-in-Aid for Scientific Research (C), 18570114 (to H.I.), from the Ministry of Education, Culture, Sports, Science and Technology of Japan and by a Grant-in-Aid for Scientific Research (C) 16570125 (to H.H.) from the Ministry of Education, Culture, Sports, Science and Technology of Japan.

REFERENCES

1. **Alexander, F. W., E. Sandmeier, P. K. Mehta, and P. Christen.** 1994. Evolutionary relationships among pyridoxal-5′-phosphate-dependent enzymes. Regio-specific alpha, beta and gamma families. Eur. J. Biochem. **219:**953–960.
2. **Alexeev, D., M. Alexeeva, R. L. Baxter, D. J. Campopiano, S. P. Webster, and L. Sawyer.** 1998. The crystal structure of 8-amino-7-oxononanoate synthase: a bacterial PLP-dependent, acyl-CoA-condensing enzyme. J. Mol. Biol. **284:**401–419.
3. **Allen, M. J., T. Forster, D. C. Schroeder, M. Hall, D. Roy, P. Ghazal, and W. H. Wilson.** 2006. Locus-specific gene expression pattern suggests a unique propagation strategy for a giant algal virus. J. Virol. **80:**7699–7705.
4. **Astner, I., J. O. Schulze, J. van den Heuvel, D. Jahn, W. D. Schubert, and D. W. Heinz.** 2005. Crystal structure of 5-aminolevulinate synthase, the first enzyme of heme biosynthesis, and its link to XLSA in humans. EMBO J. **24:**3166–3177.
5. **Ausubel, F. M., R. Brent, R. E. Kingston, D. D. Moore, J. G. Seidman, J. A. Smith, and K. Struhl.** 1994. Current protocols in molecular biology, Suppl. 27, unit 2.4. John Wiley & Sons, Inc., New York, NY.
6. **Bejaoui, K., C. Wu, M. D. Scheffler, G. Haan, P. Ashby, L. Wu, P. de Jong, and R. H. Brown, Jr.** 2001. SPTLC1 is mutated in hereditary sensory neuropathy, type 1. Nat. Genet. **27:**261–262.
7. **Bejaoui, K., Y. Uchida, S. Yasuda, M. Ho, M. Nishijima, R. H. Brown, Jr., W. M. Holleran, and K. Hanada.** 2002. Hereditary sensory neuropathy type 1 mutations confer dominant negative effects on serine palmitoyltransferase, critical for sphingolipid synthesis. J. Clin. Investig. **110:**1301–1308.
8. **Blahova, J., K. Kralikova, V. Krcmery, Sr., and K. Kubonova.** 1997. Hydrolysis of imipenem, meropenem, ceftazidime, and cefepime by multiresistant nosocomial strains of *Sphingobacterium multivorum*. Eur. J. Clin. Microbiol. Infect. Dis. **16:**178–180.
9. **Bligh, E. G., and W. J. Dyer.** 1959. A rapid method of total lipid extraction and purification. Can. J. Biochem. Physiol. **37:**911–917.
10. **Buede, R., S. C. Rinker, W. J. Pinto, R. L. Lester, and R. C. Dickson.** 1991. Cloning and characterization of LCB1, a *Saccharomyces* gene required for biosynthesis of the long-chain base component of sphingolipids. J. Bacteriol. **173:**4325–4332.
11. **Dawkins, J. L., D. J. Hulme, S. B. Brahmbhatt, M. Auer-Grumbach, and G. A. Nicholson.** 2001. Mutations in SPTLC1, encoding serine palmitoyltransferase, long chain base subunit-1, cause hereditary sensory neuropathy type I. Nat. Genet. **27:**309–312.
12. **Dedov, V. N., I. V. Dedova, A. H. Merrill, Jr., and G. A. Nicholson.** 2004. Activity of partially inhibited serine palmitoyltransferase is sufficient for normal sphingolipid metabolism and viability of HSN1 patient cells. Biochim. Biophys. Acta **1688:**168–175.
13. **Dedov, V. N., I. V. Dedova, and G. A. Nicholson.** 2004. Hypoxia causes aggregation of serine palmitoyltransferase followed by non-apoptotic death of human lymphocytes. Cell Cycle **3:**1271–1277.
14. **Dykstra, M., A. Cherukuri, H. W. Sohn, S. J. Tzeng, and S. K. Pierce.** 2003. Location is everything: lipid rafts and immune cell signaling. Annu. Rev. Immunol. **21:**457–481.
15. **Ferreira, G. C., and J. S. Zhang.** 2002. Mechanism of 5-aminolevulinate synthase and the role of the protein environment in controlling the cofactor chemistry. Cell Mol. Biol. **48:**827–833.
16. **Freney, J., W. Hansen, C. Ploton, H. Meugnier, S. Madier, N. Bornstein, and J. Fleurette.** 1987. Septicemia caused by *Sphingobacterium multivorum*. J. Clin. Microbiol. **25:**1126–1128.
17. **Gable, K., G. Han, E. Monaghan, D. Bacikova, M. Natarajan, R. Williams, and T. M. Dunn.** 2002. Mutations in the yeast LCB1 and LCB2 genes, including those corresponding to the hereditary sensory neuropathy type I mutations, dominantly inactivate serine palmitoyltransferase. J. Biol. Chem. **277:**10194–101200.
18. **Han, G., K. Gable, L. Yan, M. J. Allen, W. H. Wilson, P. Moitra, J. M. Harmon, and T. M. Dunn.** 2006. Expression of a novel marine viral single-chain serine palmitoyltransferase and construction of yeast and mammalian single-chain chimera. J. Biol. Chem. **281:**39935–39942.
19. **Hanada, K., T. Hara, M. Nishijima, O. Kuge, R. C. Dickson, and M. M. Nagiec.** 1997. A mammalian homolog of the yeast LCB1 encodes a component of serine palmitoyltransferase, the enzyme catalyzing the first step in sphingolipid synthesis. J. Biol. Chem. **272:**32108–32114.
20. **Hanada, K., T. Hara, and M. Nishijima.** 2000. Purification of the serine palmitoyltransferase complex responsible for sphingoid base synthesis by using affinity peptide chromatography techniques. J. Biol. Chem. **275:**8409–8415.
21. **Hanada, K.** 2003. Serine palmitoyltransferase, a key enzyme of sphingolipid metabolism. Biochim. Biophys. Acta **1632:**16–30.
22. **Hannun, Y. A., and C. Luberto.** 2000. Ceramide in the eukaryotic stress response. Trends Cell Biol. **10:**73–80.
23. **Holmes, B., R. J. Owen, and D. G. Hollis.** 1982. *Flavobacterium spiritivorum*, a new species isolated From human clinical specimens. Int. J. Syst. Bacteriol. **32:**157–165.
24. **Hornemann, T., S. Richard, M. F. Rutti, Y. Wei, and A. von Eckardstein.** 2006. Cloning and initial characterization of a new subunit for mammalian serine-palmitoyltransferase. J. Biol. Chem. **281:**37275–37281.
25. **Huwiler, A., T. Kolter, J. Pfeilschifter, and K. Sandhoff.** 2000. Physiology and pathophysiology of sphingolipid metabolism and signaling. Biochim. Biophys. Acta **1485:**63–99.
26. **Ikushiro, H., H. Hayashi, and H. Kagamiyama.** 2000. Expression and purification of serine palmitoyltransferase, p. 251–254. *In* A. Iriarte, H. M. Kagan, and M. Martinez-Carrion (ed.), Biochemistry and molecular biology of vitamin B6 and PQQ-dependent proteins. Birkhaeuser Verlag, Basel, Switzerland.
27. **Ikushiro, H., H. Hayashi, and H. Kagamiyama.** 2001. A water-soluble homodimeric serine palmitoyltransferase from *Sphingomonas paucimobilis* EY2395^T strain. Purification, characterization, cloning, and overproduction. J. Biol. Chem. **276:**18249–18256.
28. **Ikushiro, H., H. Hayashi, and H. Kagamiyama.** 2003. Bacterial serine palmitoyltransferase: a water-soluble homodimeric prototype of the eukaryotic enzyme. Biochim. Biophys. Acta **1647:**116–120.
29. **Ikushiro, H., H. Hayashi, and H. Kagamiyama.** 2004. Reactions of serine palmitoyltransferase with serine and molecular mechanisms of the actions of serine derivatives as inhibitors. Biochemistry **43:**1082–1092.
30. **Ito, M., U. Tchoua, M. Okamoto, and H. Tojo.** 2002. Purification and properties of a phospholipase A2/lipase preferring phosphatidic acid, bis(monoacylglycerol) phosphate, and monoacylglycerol from rat testis. J. Biol. Chem. **277:**43674–43681.
31. **Kallen, R. G., T. Korpela, A. E. Martell, Y. Matsushima, C. M. Metzler, D. E. Metzler, Y. V. Morozov, I. M. Ralston, F. A. Savin, Y. M. Torchinsky, and H. Ueno.** 1985. Chemical and spectroscopic properties of pyridoxal and pyridoxine phosphates, p. 37–108. *In* P. Christen and D. E. Metzler (ed.), Transaminases. John Wiley & Sons, New York, NY.
32. **Karlsson, K. A.** 1970. On the chemistry and occurrence of sphingolipid long-chain bases. Chem. Phys. Lipids **5:**6–43.
33. **Kawasaki, S., R. Moriguchi, K. Sekiya, T. Nakai, E. Ono, K. Kume, and K. Kawahara.** 1994. The cell envelope structure of the lipopolysaccharide-lacking gram-negative bacterium *Sphingomonas paucimobilis*. J. Bacteriol. **176:**284–290.
34. **Kinjo, Y., D. Wu, G. Kim, G. W. Xing, M. A. Poles, D. D. Ho, M. Tsuji, K. Kawahara, C. H. Wong, and M. Kronenberg.** 2005. Recognition of bacterial glycosphingolipids by natural killer T cells. Nature **434:**520–525.
35. **Laemmli, U. K.** 1970. Cleavage of structural proteins during the assembly of the head of bacteriophage T4. Nature **227:**680–685.
36. **Mandon, E. C., E. Ehses, J. Rother, G. van Echten, and K. Sandhoff.** 1992. Subcellular localization and membrane topology of serine palmitoyltransferase, 3-dehydrosphinganine reductase, and sphinganine N-acyltransferase in mouse liver. J. Biol. Chem. **267:**11144–11148.
37. **Manfredi, R., A. Nanetti, M. Ferri, A. Mastroianni, O. V. Coronado, and F. Chiodo.** 1999. *Flavobacterium* spp. organisms as opportunistic bacterial pathogens during advanced HIV disease. J. Infect. **39:**146–152.
38. **Mathias, S., L. A. Pena, and R. N. Kolesnick.** 1998. Signal transduction of stress via ceramide. Biochem. J. **335:**465–480.
39. **Mattner, J., K. L. Debord, N. Ismail, R. D. Goff, C. Cantu, III, D. Zhou, P. Saint-Mezard, V. Wang, Y. Gao, N. Yin, K. Hoebe, O. Schneewind, D. Walker, B. Beutler, L. Teyton, P. B. Savage, and A. Bendelac.** 2005. Exogenous and endogenous glycolipid antigens activate NKT cells during microbial infections. Nature **434:**525–529.
40. **McCampbell, A., D. Truong, D. C. Broom, A. Allchorne, K. Gable, R. G. Cutler, M. P. Mattson, C. J. Woolf, M. P. Frosch, J. M. Harmon, T. M. Dunn, and R. H. Brown, Jr.** 2005. Mutant SPTLC1 dominantly inhibits serine palmitoyltransferase activity in vivo and confers an age-dependent neuropathy. Hum. Mol. Genet. **14:**3507–3521.
41. **Nagiec, M. M., J. A. Baltisberger, G. B. Wells, R. L. Lester, and R. C. Dickson.** 1994. The LCB2 gene of *Saccharomyces* and the related LCB1 gene encode subunits of serine palmitoyltransferase, the initial enzyme in sphingolipid synthesis. Proc. Natl. Acad. Sci. USA **91:**7899–7902.
42. **Nagiec, M. M., R. L. Lester, and R. C. Dickson.** 1996. Sphingolipid synthesis: identification and characterization of mammalian cDNAs encoding the Lcb2 subunit of serine palmitoyltransferase. Gene **177:**237–241.
43. **Naka, T., N. Fujiwara, S. Maeda, E. Yabuuchi, M. Doe, K. Kobayashi, Y. Kato, and I. Yano.** 2000. A novel sphingoglycolipid containing galacturonic acid and 2-hydroxy fatty acid in cellular lipids of *Sphingomonas yanoikuyae*. J. Bacteriol. **182:**2660–2663.
44. **Naka, T., N. Fujiwara, I. Yano, S. Maeda, M. Doe, M. Minamino, N. Ikeda, Y. Kato, K. Watabe, Y. Kumazawa, I. Tomiyasu, and K. Kobayashi.** 2003. Structural analysis of sphingophospholipids derived from *Sphingobacterium spiritivorum*, the type species of genus *Sphingobacterium*. Biochim. Biophys. Acta **1635:**83–92.
45. **Radin, N. S.** 1981. Preparative isolation of lecithin. Methods Enzymol. **72:**5–7.
46. **Rendulic, S., P. Jagtap, A. Rosinus, M. Eppinger, C. Baar, C. Lanz, H. Keller, C. Lambert, K. J. Evans, A. Goesmann, F. Meyer, R. E. Sockett, and S. C. Schuster.** 2004. A predator unmasked: life cycle of *Bdellovibrio bacteriovorus* from a genomic perspective. Science **303:**689–692.
47. **Ruby, E. G.** 1991. The genus *Bdellovibrio*, p. 3400–3415. *In* A. Balows, H. G.

Trüper, M. Dworkin, W. Harder, and K. H. Schleifer (ed.). The prokaryotes. A handbook on the biology of bacteria: ecophysiology, isolation, identification, applications, 2nd ed. Springer-Verlag, New York, NY.

48. **Schmidt, A., J. Sivaraman, Y. Li, R. Larocque, J. A. Barbosa, C. Smith, A. Matte, J. D. Schrag, and M. Cygler.** 2001. Three-dimensional structure of 2-amino-3-ketobutyrate CoA ligase from *Escherichia coli* complexed with a PLP-substrate intermediate: inferred reaction mechanism. Biochemistry **40:** 5151–5160.
49. **Segel, I. H.** 1975. Steady state kinetics of multireactant enzymes. *In* Enzyme kinetics, p. 505–515. John Wiley & Sons, Inc., New York, NY.
50. **Seo, J. S., H. Chong, H. S. Park, K. O. Yoon, C. Jung, J. J. Kim, J. H. Hong, H. Kim, J. H. Kim, J. I. Kil, C. J. Park, H. M. Oh, J. S. Lee, S. J. Jin, H. W. Um, H. J. Lee, S. J. Oh, J. Y. Kim, H. L. Kang, S. Y. Lee, K. J. Lee, and H. S. Kang.** 2005. The genome sequence of the ethanologenic bacterium *Zymomonas mobilis* ZM4. Nat. Biotechnol. **23:**63–68.
51. **Shivaji, S., M. K. Ray, N. S. Rao, L. Saisree, M. V. Jagannadham, G. S. Kumar, G. S. N. Reddy, and P. M. Bhargava.** 1992. *Sphingobacterium antarcticus* sp. nov., a psychrotrophic bacterium from the soils of Schirmacher Oasis, Antarctica. Int. J. Syst. Bacteriol. **42:**102–106.
52. **Simons, K., and E. Ikonen.** 1997. Functional rafts in cell membranes. Nature **387:**569–572.
53. **Snell, E. E., S. J. Dimari, and R. H. Brady.** 1970. Biosynthesis of sphingosine and dihydrosphingosine by cell-free systems from *Hansenula ciferri*. Chem. Phys. Lipids **5:**116–138.
54. **Spiegel, S., and A. H. Merrill, Jr.** 1996. Sphingolipid metabolism and cell growth regulation. FASEB J. **10:**1388–1397.
55. **Sriram, V., W. Du, J. Gervay-Hague, and R. R. Brutkiewicz.** 2005. Cell wall glycosphingolipids of *Sphingomonas paucimobilis* are CD1d-specific ligands for NKT cells. Eur. J. Immunol. **35:**1692–1701.
56. **Steiner, S., S. F. Conti, and R. L. Lester.** 1973. Occurrence of phosphonosphingolipids in *Bdellovibrio bacteriovorus* strain UKi2. J. Bacteriol. **116:** 1199–1211.
57. **Stolp, H., and P. Starr.** 1963. Bdellovibrio bacteriovorus gen. et sp. n., a predatory, ectoparasitic, and bacteriolytic microorganism. Antonie Leeuwenhoek J. Microbiol. Serol. **29:**217–248.
58. **Takagi, S., H. Tojo, S. Tomita, S. Sano, S. Itami, M. Hara, S. Inoue, K. Horie, G. Kondoh, K. Hosokawa, F. J. Gonzalez, and J. Takeda.** 2003. Alteration of the 4-sphingenine scaffolds of ceramides in keratinocyte-specific Arnt-deficient mice affects skin barrier function. J. Clin. Investig. **112:** 1372–1382.
59. **Thompson, J. D., T. J. Gibson, F. Plewniak, F. Jeanmougin, and D. G. Higgins.** 1997. The CLUSTAL_X windows interface: flexible strategies for multiple sequence alignment aided by quality analysis tools. Nucleic Acids Res. **25:**4876–4882.
60. **Tronel, H., P. Plesiat, E. Ageron, and P. A. Grimont.** 2003. Bacteremia caused by a novel species of *Sphingobacterium*. Clin. Microbiol. Infect. **9:**1242–1244.
61. **Verhoeven, K., K. Coen, E. De Vriendt, A. Jacobs, V. Van Gerwen, I. Smouts, A. Pou-Serradell, J. J. Martin, V. Timmerman, and P. De Jonghe.** 2004. SPTLC1 mutation in twin sisters with hereditary sensory neuropathy type I. Neurology **62:**1001–1002.
62. **Watanabe, Y., M. Nakajima, T. Hoshino, K. Jayasimhulu, E. E. Brooks, and E. S. Kaneshiro.** 2001. A novel sphingophosphonolipid head group 1-hydroxy-2-aminoethyl phosphonate in *Bdellovibrio stolpii*. Lipids **36:**513–519.
63. **Webster, S. P., D. Alexeev, D. J. Campopiano, R. M. Watt, M. Alexeeva, L. Sawyer, and R. L. Baxter.** 2000. Mechanism of 8-amino-7-oxononanoate synthase: spectroscopic, kinetic, and crystallographic studies. Biochemistry **39:**516–528.
64. **Weiss, B., and W. Stoffel.** 1997. Human and murine serine-palmitoyl-CoA transferase—cloning, expression and characterization of the key enzyme in sphingolipid synthesis. Eur. J. Biochem. **249:**239–247.
65. **Wilson, W. H., D. C. Schroeder, M. J. Allen, M. T. Holden, J. Parkhill, B. G. Barrell, C. Churcher, N. Hamlin, K. Mungall, H. Norbertczak, M. A. Quail, C. Price, E. Rabbinowitsch, D. Walker, M. Craigon, D. Roy, and P. Ghazal.** 2005. Complete genome sequence and lytic phase transcription profile of a Coccolithovirus. Science **309:**1090–1092.
66. **Wu, D., G. W. Xing, M. A. Poles, A. Horowitz, Y. Kinjo, B. Sullivan, V. Bodmer-Narkevitch, O. Plettenburg, M. Kronenberg, M. Tsuji, D. D. Ho, and C. H. Wong.** 2005. Bacterial glycolipids and analogs as antigens for CD1d-restricted NKT cells. Proc. Natl. Acad. Sci. USA **102:**1351–1356.
67. **Yabuuchi, E., E. Tanimura, Y. Kosako, A. Ohyama, I. Yano, and A. Yamamoto.** 1979. Flavobacterium devorans ATCC 10829: a strain of Pseudomonas paucimobilis. J. Gen. Appl. Microbiol. **25:**95–107.
68. **Yabuuchi, E., I. Yano, H. Oyaizu, Y. Hashimoto, T. Ezaki, and H. Yamamoto.** 1990. Proposals of *Sphingomonas paucimobilis* gen. nov. and comb. nov., *Sphingomonas parapaucimobilis* sp. nov., *Sphingomonas yanoikuyae* sp. nov., *Sphingomonas adhaesiva* sp. nov., *Sphingomonas capsulata* comb. nov., and two genospecies of the genus *Sphingomonas*. Microbiol. Immunol. **34:**99–119.
69. **Yabuuchi, E., T. Kaneko, I. Yano, C. W. Moss, and N. Miyoshi.** 1983. *Sphingobacterium gen.* nov., *Sphingobacterium spiritivorum* comb. nov., *Sphingobacterium multivorum* comb. nov., *Sphingobacterium mizutae* sp. nov., and *Flavobacterium indologenes* sp. nov.: glucose-nonfermenting gram-negative rods in CDC groups IIK-2 and IIb. Int. J. Syst. Bacteriol. **33:**580–598.
70. **Yamamoto, A., I. Yano, M. Masui, and E. Yabuuchi.** 1978. Isolation of a novel sphingoglycolipid containing glucuronic acid and 2-hydroxy fatty acid from *Flavobacterium devorans* ATCC 10829. J. Biochem. (Tokyo) **83:**1213–1216.
71. **Yano, I., I. Tomiyasu, and E. Yabuuchi.** 1982. Long chain base composition of strains of three species of *Sphingobacterium* gen. nov. FEMS Microbiol. Lett. **15:**303–307.
72. **Yano, I., S. Imaizumi, I. Tomiyasu, and E. Yabuuchi.** 1983. Separation and analysis of free ceramides containing 2-hydroxy fatty acids in *Sphingobacterium* species. FEMS Microbiol. Lett. **20:**449–453.

第20章　自動化脂質分析装置を用いた病態リピドミクス

東城博雅*

1　はじめに

本書の主題であるメタボロミクスは多種多様な代謝中間体の総覧的な分析に基づき生体機能を論ずる学問である。広範な物性スペクトルを示す代謝中間体のうち，水に不溶な低極性化合物群からなる脂質は生体膜の骨格，膜蛋白質の機能的構成成分，細胞内外でのシグナル伝達分子などとして重要な分子である。脂質のメタボロミクスは，最近，脂質関係の国際学会やジャーナルではリピドミクスと呼ばれることが多く，その重要性が注目されている。リピドミクスにおける質量分析（MS）の利用法と問題点については，最近，総説[1]や教科書[2]に詳述した。本稿では筆者が開発して関連の大学発ベンチャー会社・オムニセパロ適塾（OmniSeparo-TJ, Inc. OSTJ）で研究や商業途用に改良を進めている高速液体クロマトグラフィー（HPLC)/MSを用いた自動化脂質分析システムの概要と病態リピドミクスへの応用について概説する。

2　リピドミクスとプロテオミクスの連携

リピドミクスで扱う（本稿では動物に存在するものに限るが）脂質は多様であるが，脂質生合成経路と密接に関連した化学構造の特徴に基づき単純脂質と複合脂質に大別して理解すると便利である（図1)。単純脂質は炭素，水素，酸素のみからなり，脂肪酸（活性型はアシルCoA）とその酸化誘導体（エイコサノイドなど)，イソプレノイド類に属するコレステロールやその誘導体ステロイドホルモンなどが含まれる。必須脂肪酸（リノール酸，α-リノレン酸）やイソプレノイド類ビタミン以外のこれらの脂質は解糖系からクエン酸回路への中継点にあるアセチルコエンザイムA（CoA）を利用して生合成される。単純脂質は複合脂質の構成成分でもある。複合脂質は，リン，窒素，硫黄など異核原子も含み，グリセロール骨格を含むグリセロ脂質あるいはスフィンゴシンを主成分とする長鎖塩基骨格を含むスフィンゴ脂質に分けられる。グリセロール骨格（グリセロール-3-リン酸）は解糖系中間体のジヒドロキシアセトンリン酸から作られ，脂肪酸が縮合したのちにグリセロリン脂質の極性頭基（ホスホコリンなど）形成・交換やトリアシ

* Hiromasa Tojo　大阪大学　大学院医学系研究科　分子医化学　准教授

種類	特徴	基本骨格
1. 単純脂質	脂肪酸と誘導体，ステロイド(イソプレノイド)などC,H,Oからなりアセチル CoAから生合成される。複合脂質の構成成分でもある。	
2. 複合脂質	異核元素N,P,Sなども含み膜脂質の主要成分	
グリセロ脂質	グリセロリン脂質 グリセロ糖脂質 アシルグリセロール	グリセロール 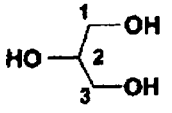
スフィンゴ脂質	スフィンゴリン脂質 スフィンゴ糖脂質	スフィンゴシン 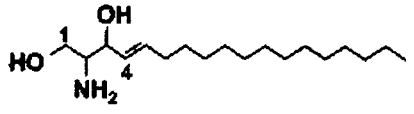

図1　リピドミクスの理解に便利な脂質の分類
生合成過程では4位に二重結合のないスフィンガニンが合成されその後修飾を受ける。これらの骨格には2位に塩基であるアミノ基があるので総称して長鎖塩基あるいはスフィンゴイド塩基と呼ばれる。文献2）から改変。

ルグリセロール合成などが起こり，全てのグリセロ脂質が合成される。一方，長鎖塩基骨格はジヒドロキシアセトンリン酸の少し下流の解糖系中間体3-ホスホグリセリン酸から合成されるセリンとアシル CoA からスフィンガニンとして作られ，脂肪酸が縮合したのち塩基骨格の修飾や糖の縮合が起こり，スフィンゴ脂質が合成される。

このように脂質デノボ合成は二つの解糖系中間体とアセチル CoA を介して起こり，解糖系とクエン酸回路の3から5個の炭素からなる代謝中間体を介して複雑に連携する糖・アミノ酸代謝と比較すると閉じた代謝系を形成する。脂質分解系における代謝中間体も糖・アミノ酸代謝に帰るものは少ない。複合脂質から加水分解酵素作用で遊離した脂肪酸は完全酸化され二酸化炭素になる。複合脂質骨格のうちグリセロールは肝臓・腎臓での糖新生によりグルコースに再変換可能であるが，極性頭基を形成するコリン，イノシトールなどは食事から摂取する必要がある必須栄養素で再利用され，エタノールアミンはセリンから脂質代謝系内で生成され再利用される。ちなみに，コリンのヒトでの生成系は，おもに肝臓で起こるホスファチジルエタノールアミン（PE）の段階的メチル化によるホスファチジルコリン（PC）中のコリン残基の合成だけである。スフィンゴシン骨格は分解されるとホスホエタノールアミンと長鎖アルデヒドになるが前者は脂質代謝内で再利用され，後者は酸化されると脂肪酸酸化系に入り完全酸化され得る。また，マクロファージなど細胞膜の代謝回転が速い細胞では，デノボ合成が間に合わないので膜脂質を盛んに再利用する。脂質分解系のもう一つの重要な機能は，多彩な脂質性シグナル分子や生理活性脂質

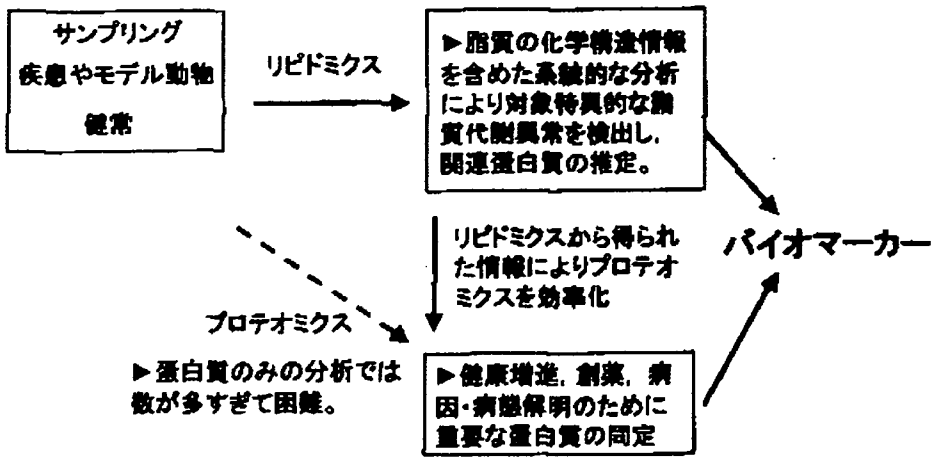

図2　リピドミクスとプロテオミクスの連携

を産生することである[1,2]。小胞体シトゾール側でデノボ合成されたリン脂質中の特に *sn*-2 位脂肪酸は，多くの場合リモデリング酵素系によりすげ替えられ鎖長・不飽和度が変更され，目的の細胞内小器官膜に輸送される。これらの膜脂質から刺激に応答したホスホリパーゼ等の酵素作用で脂質性シグナル分子前駆体やシグナル分子自身が遊離される。前駆体は，酸化（酸素添加），過酸化，極性頭基イノシトールやスフィンゴシンの（ポリ）リン酸化，極性頭基の修飾などほとんどの場合脂質代謝系内（ペプチドや糖の付加などを除いて）で行われる反応によりシグナル分子になる。

以上のように，脂質代謝は他の代謝系と代謝中間体相互の連携が少ないため，リピドミクスから得られた脂質組成異常情報から関連酵素や蛋白質を推測しやすくプロテオミクス解析の効率化を助けることができる。実際，以下に述べる自動化装置を用いて検出した脂質組成異常から病態関連蛋白質を同定できた例を報告した[3]。また，プロテオミクスや分子生物学的解析では，上記のシグナル分子の下流で起こるすべての変化が反映され解析が複雑になるが，シグナル分子の変動を直接解析し刺激応答経路のより上流の情報を得られるリピドミクスを併用すると解析を効率化できる。ただし，一般的なリピドミクス解析では，定常状態での組織内脂質濃度変化を測定するので，さらに直接的な刺激応答経路の脂質組成変動を調べるためには，安定同位体標識脂質前駆体などを用いた脂質組成変化のカイネティックスを調べる研究などを追加する必要がある。

このようなリピドミクスの特徴を生かした解析を促進するため，筆者のグループでは，一つの組織，細胞，単離した細胞内小器官膜画分などのサンプルから出発してまず脂質を抽出して残りの残渣にある蛋白質を効率よく加水分解してリピドミクスとプロテオミクス解析する方法の開発を進めている（図2）。ここで問題になるのは，脂質が水にまったく溶けない非極性のものからミセルとして完全に溶解するものまで高範囲な極性スペクトルを示すため，全ての脂質を一度に

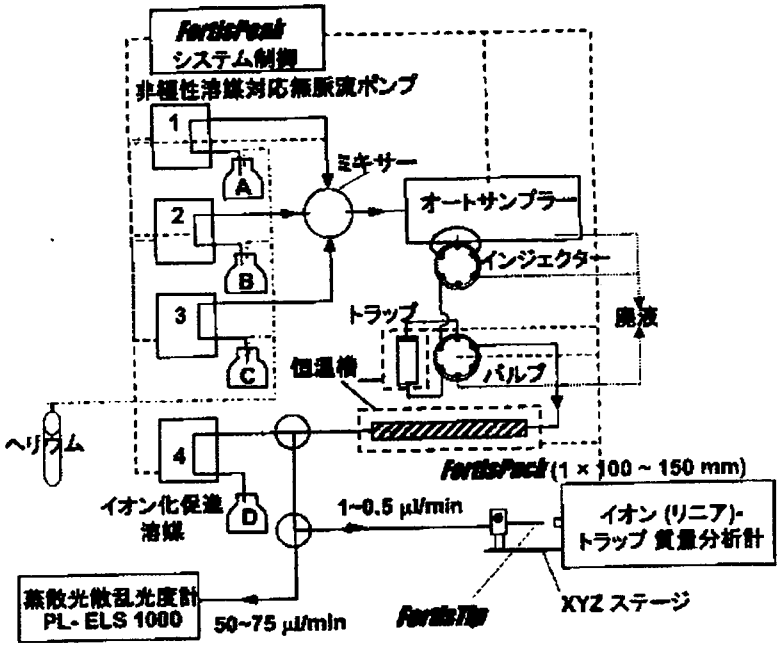

図3　自動化脂質分析装置の概略図

抽出する方法は現在のところ存在しないこと，疎水性蛋白質がかなりの量抽出脂質画分に混入してくることである。定法の Folch 法や Bligh-Dyer 法で抽出した脂質には，非極性脂質とリン脂質が主に含まれるが，高極性の脂質の回収率は悪い。高極性脂質クラスはその物性に従った適当な方法で再抽出することが必要であるがその画分には蛋白質の混入が多い。本稿では，Folch 法などで抽出した脂質に含まれる各脂質クラスの分子種（構成脂肪酸の鎖長・二重結合数）組成を効率よく比較するリピドミクス解析方法について述べる。現在，この極性範囲の脂質は，後述の自動化装置と抽出法の最適化により安定してデータを取れるようになっている。この方法によるリピドミクスと平行して行った病態プロテオミクスに関するデータは，別の機会に紹介する。

3　中性脂質からリン脂質にわたる極性の脂質クラスの自動化分析装置

薄層クロマトグラフィー（TLC）と同様に脂質を低極性のものから順に極性に従いクラス分離できる（誘導体化）シリカゲルを用いる順相 HPLC により，コレステロールエステルからリゾ PC にわたる極性範囲の脂質クラスを一回のクロマトグラフィーで分離できる。図3に示す装置の概略のように，3溶媒グラディエント HPLC システム（ポンプ 1-3）を使用する[1, 2, 4]。この HPLC システムをエレクトロスプレイイオン化（ESI）を用いた MS 装置に接続するためには，HPLC の分離能以外にイオン化効率を保つ溶媒系が必要であり，ヘキサン/2-プロパノールをベースにした溶媒系を開発し使用している。順相カラムとして高感度化だけが必要な場合はプロ

テオミクス解析と同様にキャピラリーカラムも使用できるが，実用的な耐用性があり測定感度的にも妥協できる内径1mmのFortisPack（OmniSeparo-TJ）を用いている。トラップカラムは，分離用カラムを保護するガードカラムとして，あるいはリン脂質だけや中性脂質だけを測定したい場合に不要部分を除くために使用する[5,6]。1mm内径のカラムに適した，50μl/min以下の流速でヘキサンのような非極性低粘性溶媒を安定して送液でき，かつ接液部から分析を妨害する成分が溶出しないような無脈流ポンプを開発して実装している。カラム平衡化用初期溶媒Aは～100%のヘキサンであるので電気伝導性がなくそのままではESIができないので，分析開始後約30分間は10～20mM程度のギ酸アンモニウムを含むアルコール(溶媒D)をポンプ4から送液し，カラム出口に設置したティーを介して混合してイオン化を促進する。この条件では，多くの場合中性脂質はアンモニウムイオン付加体として，セラミドはプロトン付加型として効率よく正イオン化される。さらに流路を二方向に分け一方を約1μl/minの流速でプロテオミクス解析に使用するキャピラリーHPLCとの接続用に開発した超撥水性ESIチップFortisTip（OmniSeparo-TJ）に導き[7]，他方を目的により廃棄するか蒸散光散乱光度計（ELS）に導き測定する。ELSはMSと比べると低感度であるが，脂質のうち多量成分であるコレステロールエステル，コレステロール，トリアシルグリセロール，PCなどが検出できる場合が多く，多量成分の総量の検定やESIでイオン化しにくいコレステロールの検出に役立つことがある。

現在，作動原理の異なる数種の質量分析計が市販されているが，いずれも非常に高価であり個々の研究室で購入することは簡単ではないので，各研究者の所属施設で利用可能なMS装置を使用しなければならないことも多い。筆者は所属している医学系研究科の共同利用施設に設置されていた関係でThermo Fisher Scientific社のイオントラップ型装置を使用し始めた。この装置は，加熱キャピラリーによるイオン取り込みやノイズの制御，オートゲインコントロールによるイオントラップへのイオン取り込み量の制御，タンデム質量分析（MS/MS）における質量電荷比（m/z）に依存するエネルギーの自動制御などの恩恵でHPLCとの接続性が非常によく，最適化すれば全溶出範囲にわたり非常に高感度なMSスペクトルとMS/MSスペクトルを自動的に安定して測定できるので，HPLC分離を重視する筆者等のシステムに好都合である。そのため本自動化装置でもイオン（リニアー）トラップ型装置を採用して最適化を進めた。イオン（リニアー）トラップ型装置では，MS/MSで生成するプロダクトイオンに対してMS/MSスキャンを繰り返す多段階MS/MS（MS^n）スキャン機能があり構造決定に利用できる。ある保持時間にカラムから溶出してきた脂質分子種混合物のMSスペクトルから，あらかじめ設定した閾値よりシグナル強度が大きいイオンを抽出し，強度の強いピークから順に複数の分子種のMS/MSやMS^nスペクトルを測定するデータ依存的MS/MSあるいはMS^nスキャンにより分子種組成分析を効率化できる[2]。また，交互に正負極性を切り替えながらどちらかの極性のデータ依存的MS^nスキャンを